AN ANALYSIS OF
INDENTATION OF BRITTLE MATERIALS

By

VENKATA CHANDRA MOULI VISSA

Bachelor of Engineering

Andhra University

Vishakapatnam, (A.P) India

1986

Submitted to the Faculty of the
Graduate College of the
Oklahoma State University
in partial fulfillment of
the requirements for
the Degree of
MASTER OF SCIENCE
December, 1992

Oklahoma State Univ. Library

AN ANALYSIS OF

INDENTATION OF BRITTLE MATERIALS

Thesis Approved

R Commander

Thesis Adviser

Don A. Lucca

J C. Glean

Thomas C. Collins

Dean of the Graduate College

PREFACE

Indentation is a method by which the deformation of ductile materials under point loads is studied. In recent times this technique has been extended to study the deformation and fracture of brittle materials such as advanced ceramics and glasses. Such studies have been found to be a useful precursor to the study of the mechanics of ultra-precision machining.

In this thesis, the existing analytical methods correlating the indentation parameters with material properties have been critically reviewed with a view to apply to such brittle materials as advanced ceramics. A modification to the existing analytical solution, namely Hill's spherical cavity solution has been proposed in view of the presence of high hydrostatic stress during indentation. Along with the analytical solution, finite element analysis of the elasto-plastic indentation problem has also been carried out using the CRAY Super Computer at National Center for Super Computing Applications, Chicago. Some of the results for indentation of glass have been compared with those in the technical literature and found to be in good agreement.

I wish to take the opportunity to express my sincere gratitude to all the people who assisted me in this research. In particular, I would like to thank my advisor Dr. R. Komanduri, without whose help, guidance, and encouragement this research would not have been possible. I am also deeply indebted to my committee members Dr. D.A. Lucca and Dr. Y.C. Shiau for their contributions towards the completion of this project. The help extended by Dr. Bi Zhang, Mr Ali Noori-Khajavi and Mr. Yong Wie Seo is also gratefully

acknowledged. I would also like to thank all my other research associates who have helped me in various ways.

The project was supported by a grant from the Oklahoma Center for Integrated Design and Manufacturing (OCIDM). The author is grateful for this support.

Lastly I would like to thank my parents and sister for their love, help, and encouragement.

TABLE OF CONTENTS

Chapter Page

I. INTRODUCTION 1

II. REVIEW AND ANALYSIS OF THE INDENTATION PROCESS 7

Methods of Analysis 9
Slip-line Field Theory 9

III. LITERATURE REVIEW

Ductile and Brittle Materials 14
Deformation Under Pointed and Moving Loads in Brittle Materials 17
Crack Nucleation in Indentation Process 18
Plasticity in Brittle Materials 19
Special Reference to Glass 27
Densification 31

IV. ANALYTICAL SOLUTION OF THE ELASTO-PLASTIC INDENTATION PROBLEM 34

Hill's Spherical Cavity Solution 36
Calculation of Strains 43
Correlating Hill's Solution with Indentation Parameters 45

V. MODIFIED HILL'S SPHERICAL CAVITY SOLUTION FOR INDENTATION OF BRITTLE MATERIALS 48

Yield Criterion 50
Hill's Solution with Modified a Yield Criterion 53

VI. FINITE ELEMENT ANALYSIS OF INDENTATION.....58

Formulation.....58

VII CONCLUSIONS AND RECOMMENDATIONS.....76

REFERENCES.....79

LIST OF TABLES

Table Page

3.1 Classification of Materials....16

4.1 E/Y Values of some Brittle Materials....36

6.1 Material Parameters B and Z for Various Materials 74

LIST OF FIGURES

Figure		Page
1.1	Microgrinding Regime (after Miyashata)	3
1.2	Effect of Tool Edge Radius at Micron and Submicron Machining	5
2.1	Vicker's Pyramidal Indenter	9
2.2	Slip line in Indentation (a) Without Friction and (b) With Friction	13
3.1	Shear Displacement of one Plane of Atoms over Another	15
3.2	Flow and Crack Initiation Beneath a Moving Indenter	20
3.3	Schematic of Crack Formation Under Pointed Load	21
4.1	Elasto-Plastic Solution of the Indentation Problem	37
4.2	Stress Diagram for a Spherical Element	39
4.3	Johnson's Model for Correlating Indentation Parameters with Hill's Spherical Cavity Solution	46
5.1	Effect of Hydrostatic Pressure on Stress-Strain Curve	49
6.1	Finite Element Mesh used for Indentation problem	60
6.2	Direction of Material Flow in Indentation of Glass at 10μm depth of Indentation	62
6.3	Contours of Hydrostatic Pressure in Indentation of Glass at 10μm depth of Indentation	63
6.4	Variation of the Maximum Principal Stress Along the axis of Indentation in Indentation of Glass for $\beta=45°$	64

Figure Page

6.5 Variation of the Maximum Principal Stress Along the Axis of Symmetry in Indentation of Glass for β=45°.....65

6.6 Variation in the Maximum Principal Stress with Depth of Indentation for Glass β=22°.....66

6.7 Variation in the Maximum Principal Stress for Various Ductile Materials (β=22°) at a Depth of indentation of 1μm.....67

6.8 Variation in the Maximum Principal Stress in indentation of Glass at Various Depths (after Franse).....68

6.9 Variation in the Hydrostatic Stress Along the Axis of Symmetry for Various Brittle Materials (β=22°) at 1μm Depth of Indentation.....70

6.10 Variation in the Hydrostatic Pressure Along the Axis of Indentation for various Ductile Materials (β=22°) at 1μm Depth of Indentation 71

6.11 Variation in the Hydrostatic Stress Along the Axis of Indentation in various Ductile and Brittle Materials (β=22°) at 1μm Depth of indentation.....72

6.12 P/Y Versus Material constants B and Z.....75

CHAPTER 1

INTRODUCTION

Indentation is a method for determining the resistance of materials to deformation and is commonly used to measure hardness of materials. Over the years, indentation tests have been used not only for the measurement of hardness, but also for such varied attributes as resistance to scratching, cutting, plastic deformation, and cracking.

The concept of measurement of hardness dates back to early 1700's [1]. However, the earlier investigations only speculated on its nature. O'Neil [2] reported that the first measurement of hardness on a scientific basis was done by Reamur using the scratch method. Among the various indenters that Reamur used for his study include chisels and prisms. Vicker's indenter is one of the variants of this later tool.

With increasing use of hard materials in the early 70's, a need arose for characterizing the then newly emerging hard materials, namely, advanced ceramics. Because of its simplicity, ease of usage, and low cost indentation methods soon found wide usage for studying the "plastic" deformation as well as cracking phenomenon under varying loads. Among the various hardness measuring devices, Vicker's became the most common one, because of the following features [3] : (i) it can produce geometrically similar indentations, (ii) it can be used for small samples which are otherwise not amenable to other fracture tests, (iii) specimen preparation is not too difficult, (iv) the Vicker's indenter used to produce the hardness indentation is a standard item both on dedicated hardness testers and universal testing machines, (v) many instruments are provided with means for accurately measuring the crack lengths produced during the test, and finally, (vi) it is cost

as well as time effective.

The basic premise of the present investigation is to contribute towards the fundamental understanding on the nature of deformation that occurs beneath point loads. This, it is hoped, would throw some light on the phenomenon that underlies in the material removal process such as fine grinding. The irreversible material removal mechanisms, phenomenologically, can be divided into two classes : brittle and ductile. While the brittle mode of material removal is accompanied by nucleation and propagation of cracks, ductile regime material removal is characterized by plastic deformation. Most metals respond to processing by plastic deformation while non-metals, such as ceramics respond in the brittle mode. However, in recent times some researchers have coined a term for material removal in brittle materials at light loads as *ductile regime grinding/machining* [4]. This process of material removal has also been termed as microgrinding, a concept first put forth by Miyashata [5] who noted a gap in material removal rates between polishing and conventional grinding and termed it as microgrinding [see Figure 1.1]

Though the proponents of the ductile regime grinding theory had conducted some experiments on materials such as silicon and germanium, the evidence found thus far has not been fully conclusive in the case of fine grinding of other ceramics. Because of this, and other factors, other researchers [6] have expressed concern regarding the validity of this process in grinding of brittle materials at small depths of cut. They advanced an alternative plausible hypothesis and termed fine grinding or gentle grinding of brittle materials, at small depth of cut as gentle grinding. Here, the mechanism of material removal may still be in a brittle mode, but at low depths of cut and light loads the crack initiation at or near the surface would be small enough so as not to degrade the surface related properties of the materials. In other words, microcracks form but may not extend to the critical length where they can propagate and degrade the properties and/or performance of the materials.

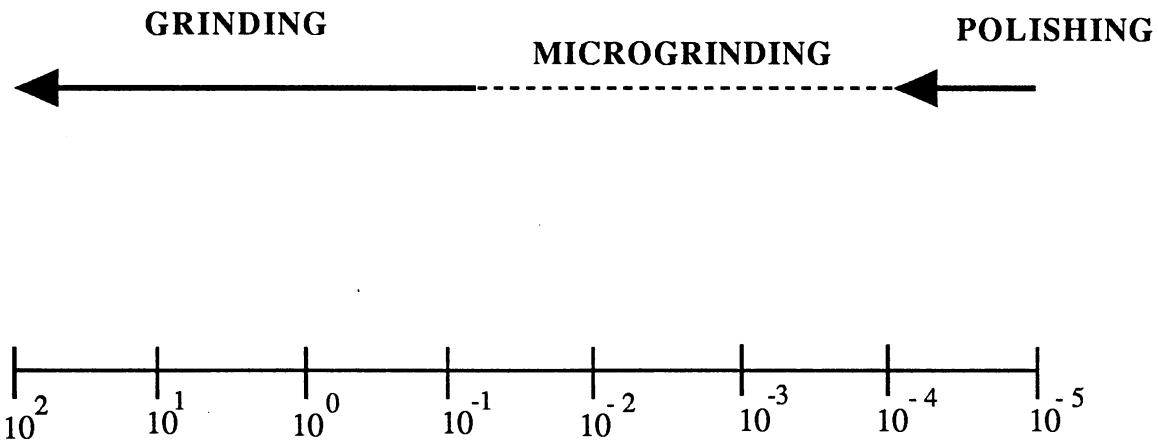

Figure 1.1 Microgrinding Regime after Miyashata [5]

Komanduri et al. [6] argue that depth of cut by itself may not dictate plasticity or brittleness of a material. Their argument is based on the following : (i) in order for a brittle material to exhibit plasticity the state of stress should be such that there is a significant component of hydrostatic pressure (almost of the order of 10MPa as reported by Bridgman [7]), (ii) in the case of either cutting or grinding, other parameters remaining the same, it does not seem that merely changing the depth of cut would result in a change of mode of deformation as the change in depth of cut alone would result in geometrically similar stresses. This implies that, merely changing the depth of cut cannot result in significant increase in hydrostatic pressure or induce ductility at the point of deformation. Komanduri, however, advanced one plausible alternate reason for the existence of ductile region in grinding at low depths of cut based on high negative rake angle of the abrasive at small depths of cut. In the case of conventional cutting, the edge radius is small and negative compared to the depth of cut. In such a case, the rake angle would be determined by the rake face. However, as the depth of cut becomes small, almost of the order of the edge radius, it becomes necessary to take into consideration the geometry of the edge radius. At these depths, the edge radius could dictate the rake angle, which will be highly negative. So, the consequence of a reduction in depth of cut could be a change in effective rake angle. This effect is schematically shown in Figure 1.2, where at large depths of cut the rake angle is the nominal rake angle as determined by the rake face while at fine depths of cut the rake angle is determined by the edge radius at the tip of the abrasive. As the rake at smaller depths of cut can be highly negative, the state of stress can change in such a way that the hydrostatic component may reach high values which can cause plastic deformation. The deformation produced by the large negative rake may be similar to that in indentation, (iii) the fact that a machined or ground surface is smooth does not necessarily mean that the surface is generated by plastic deformation. In other words, smooth surfaces can also be produced by mechanisms other than plastic flow. For instance, the smooth surface in the case of diamond is produced by cleavage and not plastic deformation, (iv) temperature

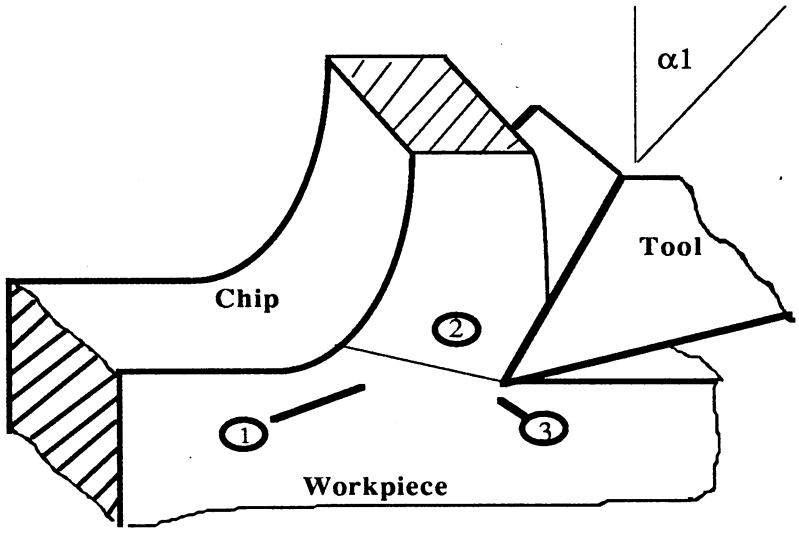

A

1. Primary Deformation Zone
2.Secondary Deformation Zone
3. Teritiary Deformation Zone

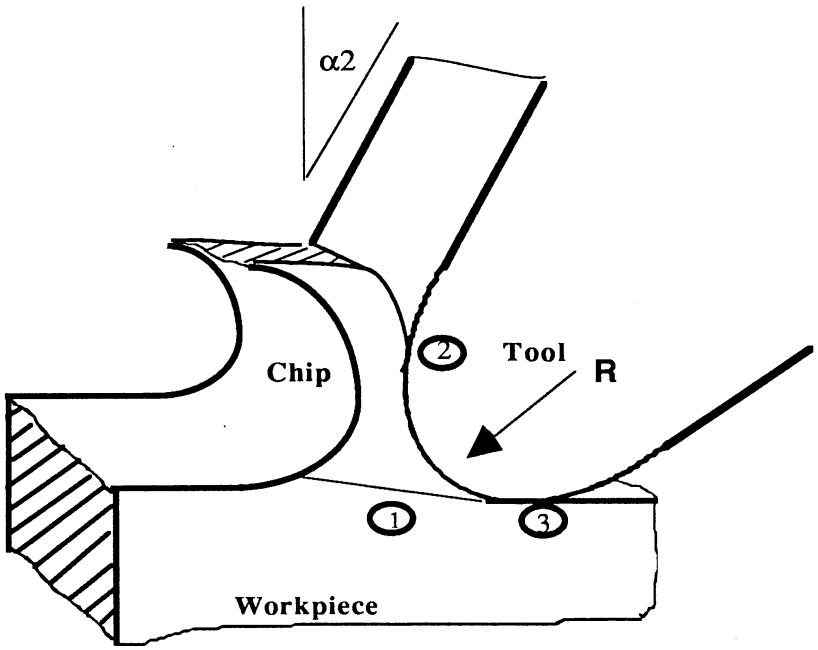

B

Figure 1.2 Effect of Tool Edge Radius at Micron and Submicron Machining

effects also play an important role. For example, in the case of glass, as the temperature increases above the glass transition temperature, it becomes viscoplastic, which when machined may produce continuous chips like the ones produced in ductile materials. The amorphous structure and viscous nature at elevated temperature, make behavior of glass different to other brittle materials such as ceramics. Hence, in the case of crystalline brittle materials with high melting temperature, such as advanced ceramics this phenomenon may not be operational at normal temperature. However, if the temperature is significantly high, then even brittle ceramics can deform plasticity.

In this research project analytical and finite element analysis of the indentation process of brittle materials are presented. In Chapter II, the indentation process and its analysis are given. Chapter III deals with a review of indentation of both brittle and ductile materials. Elaboration of the existing analytical model, namely Hill's spherical cavity solution and a modification of this model with changed yield criterion to take into account the response of brittle materials are given in Chapters IV and V respectively. Results of finite element analysis of the indentation process are discussed in Chapter VI. Finally, conclusions and recommendations are presented in Chapter VII.

CHAPTER II

REVIEW AND ANALYSIS OF THE INDENTATION PROCESS

The principle of geometric similarity is an important attribute for indentation. This principle states that if two indentations of the same geometric shape are made then, whatever their size, the strain and stress distributions will be geometrically similar. In other words, when a rigid cone, pyramid or other prismatic body indents a semi-infinite block, the shape of deformation in the material should be expected to be the same regardless of the depth [8]. This statement is valid for homogeneous materials. The important consequence of this principle is that the yield point or yield pressure measured during indentation process will be the same irrespective of the size of indentation. Of the various techniques viz Brinell, Rockwell, Knoop, and Vicker's only the later two can produce geometrically similar indentations. Because of the advantages mentioned in Chapter I and the scope of this research, Vicker's indentation technique will be briefly reviewed.

The 136^{o} diamond pyramid hardness tester commonly referred to as Vicker's indenter was first introduced by Smith and Sandland [9]. Though Vicker's indenter was initially confined to laboratories, it soon found acceptance in industry because of two factors. First, the hardness of a material is constant and independent of the load applied (except at extremely small loads). Second, and more important is the fact that this has a continuous scale from the softest to the hardest material. Also, the problem of obtaining geometrically similar impressions with different loads when using Brinell was overcome

with the introduction of Vicker's pyramidal indenter. A schematic of this indenter is shown in Figure 2.1. This indentation technique employs a sharp-pointed square pyramid made of diamond having an included angle between the faces of 136°. The 136° diamond pyramidal hardness number, usually designated as DPH is defined as the ratio of applied load to the surface area of the impression [1]

$$DPH = \frac{2L \sin\frac{\theta}{2}}{d^2} \tag{2.1}$$

where L=load. Substituting $\theta = 136°$

$$DPH = 1.854 \times \frac{load}{d^2} \tag{2.2}$$

where d is the length of the diagonal. The Vicker's hardness number H_v is related to the yield strength of the material by the equation

$$H_v = 3Y \tag{2.3}$$

An explanation for this relation in physical terms was first provided by Tabor [10]. Based on the works of Hencky and Prandtl, Tabor showed that during the indentation process about 2/3 of the applied pressure acts as hydrostatic pressure and hence does not contribute towards yielding. The remaining 1/3 pressure is what actually causes the yielding of the material. If P is taken as the mean pressure, then from the above discussion we have

$$\frac{1}{3} P = Y \text{ or } P = 3Y \tag{2.4}$$

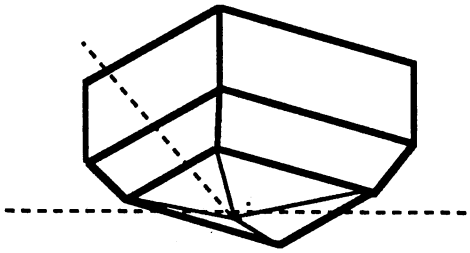

Figure 2.1 Vicker's Pyramidal Indenter

P is usually referred to as the hardness of the material.

Methods of Analysis

When a hard indenter is pressed into a material three possible situations can arise. In the first case, the resulting deformation is lower than the elastic limit of the material. The stresses and displacements then are described using the theory of elasticity. On other hand, if the deformations are large enough such that the elastic components can be neglected, it can be analyzed using the theory of plasticity, such as the slip-line filed theory. The third possible situation is when a part of the deformation is in the elastic range and a part in the plastic zone(regime). In this case, the problem becomes complex and has to be solved using tools, such as finite element analysis [11-15]. Further, the elasto-plastic indentation is also solved using modified analytical methods, such as Hill's spherical cavity solution, as will be dealt in detail in Chapter IV.

A review of the slip-line field solution of the indentation problem is given in this section. The analytical and finite element analysis of the elasto-plastic problem are given in Chapters 4 and 5 respectively.

Slip-line field theory

The first mathematical treatment of the indentation problem in terms of the slip-line field theory was given by Hill et al. [16] and subsequent to this a number of modifications have been put forth by other researchers [17]. Samuels outlined the following conditions under which the slip-line field theory can be applied to indentation [18] :

* the displacements of the points on the original surface must have a relatively large component parallel to that of the surface
* the lip of the coronet should be about 1/3 the depth of indentation
* the deformation must not extend to a considerable depth from the tip of the indenter.

Figure 2.2a shows the condition when a sharp conical indenter penetrates into a semi-infinite rigid plastic material upto a depth d, under frictionless conditions. After the penetration, three distinct zones are observed in the deformed material. In Zone 1, adjacent to the indenter, material is compressed and has yielded plastically. In zone two, the nature of deformation is complex and hence has not been described adequately. In Zone 3, the material is undeformed (elastic). When the indenter moves into the material, a coronet or a pile up will occur around the indenter. The volume of this material is equal to the volume of the material displaced by the indenter. For all values of penetration, the slip-line remains identical. With reference to Figure 2.2a the slip-line field consists of an isosceles triangle BEC, and a center face field of angle θ (angle FBE) which in turn is determined by the angle α of the indenter. Since, frictionless conditions are assumed, surface AB is assumed perfectly smooth. Consequently, it is assumed that the slip lines meet the surface at 45 °. Applying Hencky's equation yields

$$P = K\left(1 + 2\theta\right) \tag{2.5}$$

and pressure q normal to AB, is given as

$$q = K\left(1 + 2\theta\right) \tag{2.6}$$

The necessary indentation force, is therefore equal to

$$\begin{aligned} F &= 2 \times q\ AB \sin\alpha \\ &= 4k\left(1 + \theta\right) BB' \end{aligned} \tag{2.7}$$

Hence, for unit width of indenter (i.e BB'=1)

$$F = 4k\left(1 + \theta\right) \tag{2.8}$$

Considering the effect of friction, Grunzweig et al. [19], made a detailed study of indentation using the wedge type indenter and tabulated results for P/K with various included angles and coefficients of friction. When the wedge is rough, Grunzweig et al. found that the corresponding slip-line fields to deviate and no longer meet the indenter at 45 °.

If h is taken as the length of AB in Figure 2.2b, and c the depth of the penetration, then the height above the original surface is given as

$$h\cos\theta - c = \sqrt{2}h\cos\lambda \sin\left(\theta - \psi + \frac{\pi}{4} - \lambda\right) \tag{2.9}$$

From the displacement and geometric similarities

$$h\cos\left(\psi - \frac{\pi}{4} + \lambda\right) - \cos\left(\theta - \psi + \frac{\pi}{4} - \lambda\right) = \frac{\cos\theta}{\sqrt{2}\cos\lambda} \tag{2.10}$$

Using Hencky's equations and the above two relations, yields [19]

$$P = k\left(1 + 2\psi + \sin 2\lambda\right) \tag{2.11}$$

where λ and μ are related by the equation [19]

$$\mu = \frac{\cos 2\lambda}{1 + 2\mu + \sin 2\lambda} \tag{2.12}$$

A review of the slip-line field analysis for indentation in general and micro-indentation in particular was given by Samuels [18]. Based on the results of Mulheran [20] and Samuels and Mulheran [21], Samuels concluded that the cutting model of indentation (to which the slip-line field theory is applied) fails for indenters with included angle higher than 60 °. Also, he found that the discrepancy between the experimental observations and the predicted values using the slip-line theory increases for indenters with included angles above 60 ° and were pronounced at 120°. From the above, it becomes clear that the application of the slip-line field theory to indentation is limited somewhat by the geometry of the indenter.

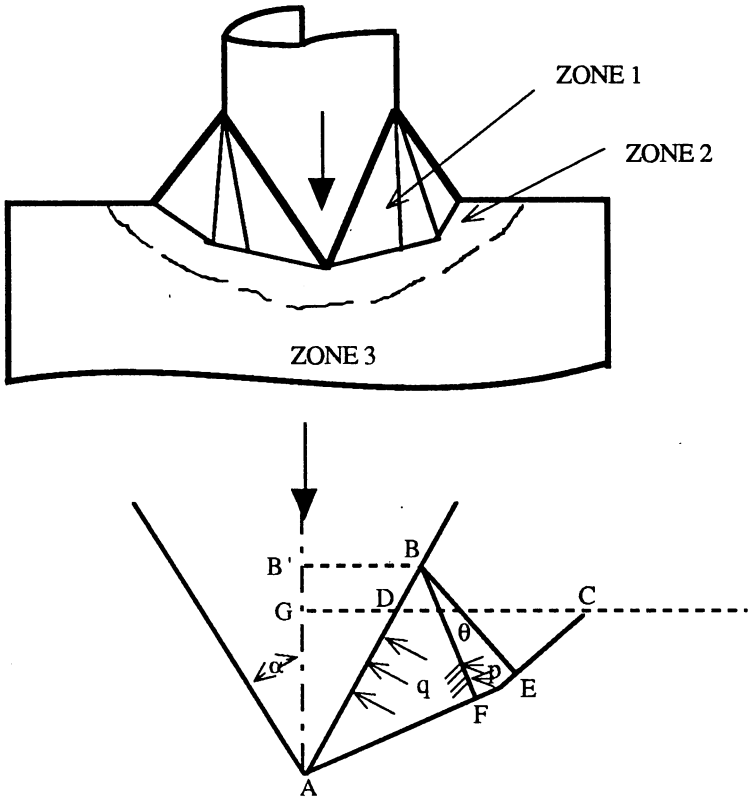

(a)

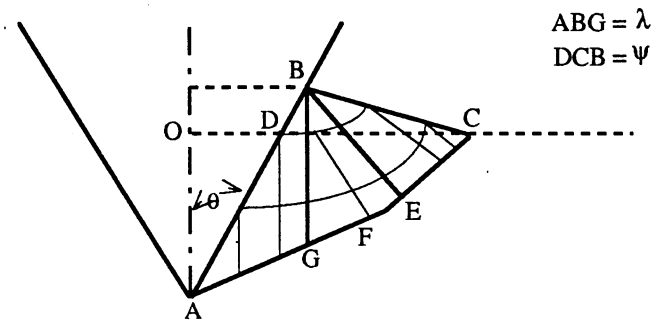

(b)

Figure 2.2 Slip line filed in indentation
(a) Without friction [17]. and (b) With friction [19]

CHAPTER III

LITERATURE REVIEW

Ductile and Brittle Materials

A solid can be formed or shaped in essentially two ways - it can be cleaved or sheared. Depending upon the energy requirements materials can be classified into brittle and ductile. If the amount of energy required to cleave is more than that required to shear then the material is ductile otherwise it is brittle. In general, the body centered cubic materials (especially metals) are usually ductile while hexagonal closed packed materials behave in a brittle manner. Two basic classification methods will be considered in this section, one from a microscopic point of view and the other from a macroscopic view.

As pointed out earlier, a useful method of classifying materials is by examining the theoretical cleavage and shear strengths. Taking a sinusoidal variation of the force, if a_0 is the equilibrium distance between two planes of atoms [see Figure 3.1] then, the maximum cleavage strength σ_{max} is given as [22]

$$\sigma_{max} = \sqrt{\frac{E\gamma}{a_0}} \tag{3.1}$$

where γ is the surface energy and E is the Young's modulus. Similarly, the theoretical shear stress (τ_{max}) is given by

$$\tau_{max} = \frac{Gb}{2\pi h} \tag{3.2}$$

where b is the repeat distance in the direction of shear and h is the distance between the atomic planes. Depending on the ratio of σ_{max}/τ_{max}, a material can be classified into either brittle or ductile solid i.e if this ratio is greater than one it is ductile otherwise it is brittle

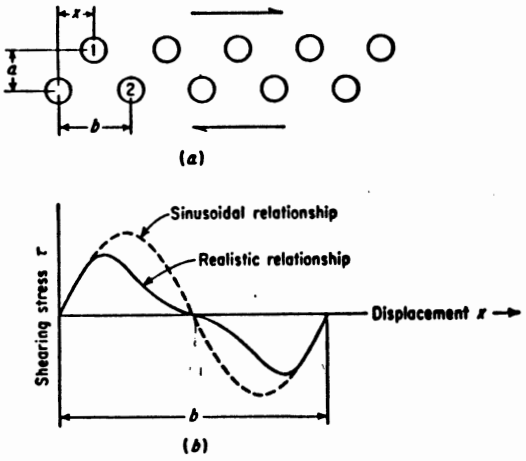

Figure 3.1 Shear displacement of one plane of atoms over another [23]

Kelly [24], based on fracture mechanics theory, defined a truly brittle material as one in which

$$\gamma_p = 2\,\gamma \qquad (3.3)$$

where, γ_p is the work done by the applied stress per unit area of fracture, γ is the specific surface free energy. A ductile crystal, on the other hand, is one in which the failure is essentially by the motion of dislocations. Another classification, also based on fracture mechanics and the motion of dislocations, has been put forth by Lawn [25] (see Table 3.1 for details). This classification is based on the nature of deformation or fracture behavior of materials.

Gogotsi et al. [26] developed a classification of materials from a macroscopic point of view. In order to characterize the mechanical behavior in quantitative terms they introduced an energetic parameter termed as brittleness, χ - which is defined as the ratio of

TABLE 3.1

CLASSIFICATION OF MATERIALS [25]

Classification	Principal Factor	Materials
Highly Brittle	Bond Rapture	Diamond, alumina, mica etc
Semi Brittle Solids	Bond Rapture & Dislocation Motion	NaCl, HCP materials, glassy Polymers etc.
Non Brittle Materials	Dislocations Motion	FCC Materials, Non-glassy polymers, most BCC materials

the specific elastic energy, U_c accumulated in the material at fracture to the whole specific energy expended to attain the limiting state.

$$\chi = \frac{\sigma^2_{lim}}{2E\int_0^{\varepsilon_{lim}} \sigma \, d\varepsilon} \tag{3.4}$$

where σ_{lim} is the strength and ε_{lim} represents the strain of the material. Brittleness ranges between $0 \leq \chi \leq 1$. Based on this definition, Gogotsi et al. classified materials as brittle and relatively brittle. Brittle materials i.e for which $\chi = 1$, are deformed without any structural change, and the point where their structure begins to change usually coincides with the point where the crack starts to emanate and move. On the other hand, relatively brittle materials are characterized by a nonlinear stress-strain behavior, which reflects the occurrence of non-elastic strains at certain stress levels.

Bridgman [27] conducted extensive studies on the fracture and flow behavior of brittle materials subjected to combined stresses involving high hydrostatic pressures. Based on this work Bridgman postulated, brittleness does not refer to the process of fracture itself but what comes prior to fracture. If a material receives a permanent set or deformation before fracture then it is termed as ductile. On the other hand, if the material fractures before experiencing any deformation it is termed as brittle. According to Bridgman, there can be only *tensile fracture or shear fracture* but not *brittle fracture.* When the term brittle fracture is used, it should be in reference to the fracture of brittle substance rather than a fracture mechanism itself. Kelly [24] pointed that many materials which are usually referred to as brittle materials may also deform in a ductile manner, under appropriate conditions. But, lack of appropriate measurement and characterizing techniques which lent credence to this classification of materials.

Kelly [24] pointed out that the line of distinction between brittle and ductile materials can be rather slim, since any crystal which cannot be cleaved must be inherently capable of propagating cracks at least at low temperatures. Materials become ductile under the conditions where the cracks are either prevented from forming and/or propagating. Therefore, it follows that the distinction between these categories can become one of conditions rather than the inherent structure and properties of the material.

Deformation Under Pointed and Moving Loads in Brittle Materials

In the previous section a brief discussion on the ductile and brittle nature of crystals was presented. In this section irreversible deformation of brittle materials such as flow, crack nucleation, and crack propagation under the action of point loads will be discussed.

The response of brittle materials under the action of point and moving loads is much different from those of ductile materials. Referring to Figure 3.2, it can be observed that

directly beneath the indenter there is a zone of irreversible deformation [28]. This zone has been referred to as plastically deformed zone, or the densified zone [29] or the microcrack zone [30] by various researchers. It is this small zone, just underneath the indenter, which may be of direct interest to the process of gentle grinding of brittle materials. Emanating from the plastic zone are two principal crack systems – the lateral cracks and the median cracks. In considering the points of origin of the crack system, the stress fields around a pointed load - namely Bossinseq stress are made use of [31]. According to this theory, the maximum tensile stress is at the specimen surface and contact axis. Hence, it appears that in all probability the cracks tend to initiate at one of these favoured locations.

Crack Nucleation in Indentation Process

The sequence of events leading to the crack formation in a brittle material during loading and unloading cycles are shown schematically in Figure 3.3 [28]. From this figure it can be seen (i) the point load produces an inelastic deformation zone just beneath the indenter, (ii) at some threshold value a deformation induced flaw will suddenly develop into a small crack- which is termed as median vent. This crack generally originates on a plane of symmetry which contains the contact axis, (iii) with increasing load, the median vent develops into a steady crack, (iv) as the load is gradually removed, the median crack will begin to close but may not heal, (v) as the unloading process continues the sideways expanding cracks referred to as lateral cracks will develop, and (vi) upon finally removing the load, the lateral cracks will extend and reach the surface and may cause chipping.

The contact problem which leads to crack nucleation in an aforesaid manner can either be a sharp object or blunt object contact. In the case of a blunt or spherical contact, the stress and subsequent cracking are modelled using Hertzian theory of contacts [25], whereas, for sharp object contact Boussinesq stress theory is used [25]. However, the basic sequence of events leading to the formation of cracks in either a sharp point contact or a spherical contact are about the same. Evans [32] observed that the stress fields that are

induced during indentation and sliding are almost similar. He argues that the essential difference between sliding process and static indentation is the presence of two extra components of the stress, namely, a compressive stress acting in front of the slider and a tensile stress acting at the trailing edge. The stress components in the plane perpendicular to the sliding direction would largely be similar to those in indentation. These stress components in a plane perpendicular to the motion of the abrasive grains in grinding are responsible for the propagation of lateral cracks, which in turn are responsible for the material removal in a brittle manner. Hence, it follows that the stresses responsible for the onset of brittle fracture in grinding could be evaluated by analyzing the stresses generated during indentation.

Plasticity in Brittle Materials

Though gentle grinding/machining of brittle materials is an emerging technology, the very concept of plasticity in brittle materials is reasonably old. The first major work in the area of plasticity in brittle materials, such as glass was conducted by Late Prof. Bridgman [7] of Harvard. Bridgman conducted a series of experiments under combined stress involving high hydrostatic pressures on a range of brittle materials such as glass, carboloy (cemented carbides), beryllium, alumina, sodium chloride, quartz and marble. When marble samples were subjected to a hydrostatic pressure of ~0.8 GPa, Bridgman [33] observed a permanent decrease in density. This increase in the volume which eventually results in a decrease in the density of the solid was observed to be a strong function of stress. Also, this component of volume increase was largely reversible and recoverable on release of the stress. However, some portion of the volume increase was irrecoverable. The interesting point is that a similar phenomenon was observed by Bridgman when AISI 1035 steel was subjected to high hydrostatic pressure. But, for steel 4/5 of the component of volume increase is relinquished when the applied stress was removed. He found that brittle materials, such as glass can be subjected to much higher

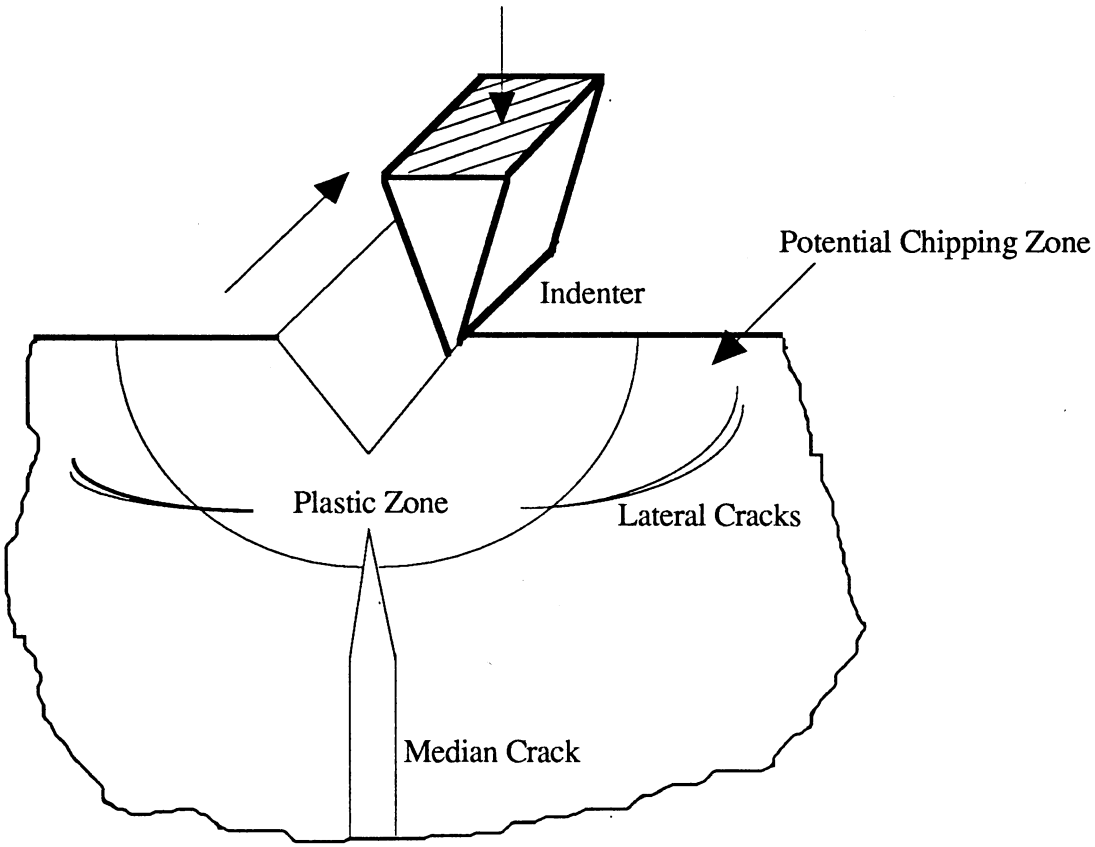

Figure 3.2 Flow and Crack Initiation Beneath a Moving Indenter [35]

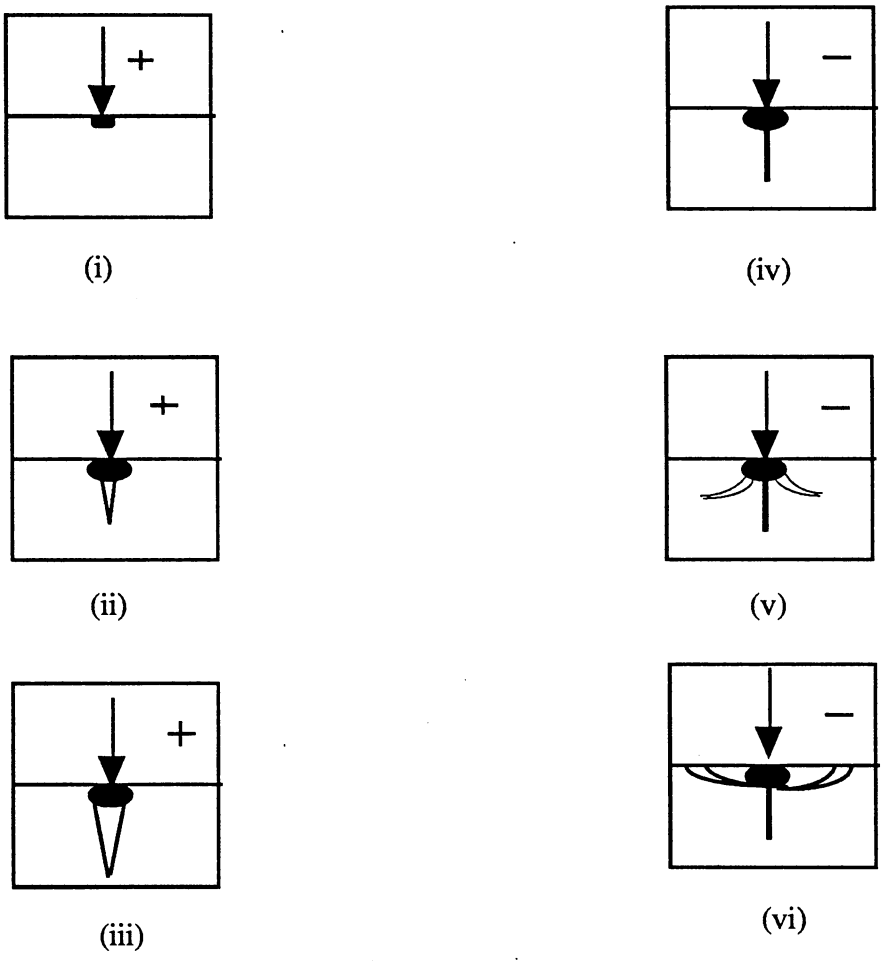

Figure 3.3 Schematic of Crack Formation Under Pointed Loads. Median Cracks are formed during the Loading (+) Cycle and the Lateral Cracks are formed during the Unloading Cycle(-) [28]

compressive stress when supported by hydrostatic pressure than by tensile stress. For instance, when glass is subjected to high hydrostatic pressures of ~ 2.7GPa, the superimposed tensile stress was around 2.4 GPa, whereas the accompanying compressive stress was around 4.5 GPa. Based on an extensive experimental investigation [27-34] on a range of brittle materials, Bridgman concluded that the entire process of fracture is an energy releasing process. Hence, energetically, tensile process is more favoured for fracture than the compressive process. Bridgman also concluded that crystalline substances, particularly cubic structure materials, lose their brittleness under that action of hydrostatic stress.

Bridgman's work was followed by some interesting work of King et al.[36]. Working on rock salt, King et al. reported plastic deformation during indentation. They classified all non-cracking, irreversible phenomenon as plastic flow. They found that under high hydrostatic pressure fracture in brittle materials was prevented and a marked plastic deformation process sets in. Under these conditions yield stress reaches a value very much greater than the bulk shear strength of the undeformed specimen. King et al. argued that since flaws and cracks act as sources of stress concentrations and play an important role in the cracking process, any method which inhibits the crack formation would lead to plasticity. Hence King attributed this "plastic" behavior in rock salt to the healing of flaws.

Though plasticity in brittle materials in general, did not draw much attention since Bridgman's monumental work, there was considerable experimental efforts on brittle geological materials were conducted. In one such study, Brace [37] observed the behavior of quartz during spherical indentation. He reported the observation of ductility during indentation, ductility referring to all non-recoverable deformation which occurs without fracture. However, Brace did not rule out the possibility of microcracking phenomenon, which according to him may not be observable. The other possible explanation for the deformation, according to Brace, was translation gliding. During this study, hardness of

quartz was found to be load dependent - i.e greater the load lesser is the hardness and vice-versa. He argued that the strength of quartz, similar to other brittle materials, could be linked to the size and distribution of flaws.

Because of their importance in manufacturing, certain carbide materials drew much attention. Starting in the 1970's most of the experiments were directed on these materials in order to study their deformation behavior as well as to characterize them in terms of their brittleness. Hertzian indentation of carbides was studied by Warren and Matzke [38]. They found that certain highly brittle carbide materials such as TiC, ZrC, VC, and NbC could not be successfully indented by a diamond indenter because of surface chipping. However, they reported that TaC indented plastically under a spherical indenter. In a similar work, on tungsten carbide, Warren [39] defined a characteristic load which he related to the crack formation and propagation. He found this characteristic load P* to be independent of the flaw size and was defined as

$$P^* = P_c = B \gamma R \tag{3.5}$$

where R is the radius of the indenting sphere, γ is the fracture surface energy and B is a constant. He observed the cracks formed close to the fracture load P_c were usually fine and often not readily detectable. However, at light loads he found these cracks became more conspicuous and multiple. At loads far greater than P_c, Warren found multiple concentric cracks.

High temperature indentation of tungsten carbide was also carried out by Rowcliffe [40]. He found the plastic flow associated with indentation process to increase with increasing temperatures. According to Rowcliffe, a prominent feature of the indentation process at room and elevated temperatures, is the difference in the shape of cracks formed. At room temperature he found the shape, was essentially circular, whereas at higher

temperature, the shape changed to hexagonal. Rowcliffe attributed this shape difference to the stress relaxation, which occurs at higher temperatures. He also found, the crack size and shape to depend more on the temperature than on load.

Certain acrylic materials also demonstrate the type of deformation seen in the case of glass and some ceramics. Puttick [41-44] carried out a series of experiments on the behavior of some brittle materials including glass, silicon, sodium chloride, and polymethylmethcralite (PMMA) during indentation. Puttick [41] studied cracking during indentation of perspex with steel balls. He found the deformation process, to be densification rather than plastic flow. Based on the changes in the refractive index of the indented material, Puttick developed an expression for the change in density under the indenter to be 3.2×10^{-3} $(d\rho/\rho)$. In a subsequent paper, Puttick [42] developed an analytical solution of the indentation of PMMA. This analysis assumed the material to have a linear stress-strain behavior in the true yield region and subsequent zero work hardening. He modelled the stress state along the lines of Hill's spherical cavity solution which is discussed in detail in Chapter IV. Puttick found the hardness of PMMA to be function of the testing rate and the material yield stress a function of the strain rate and the hydrostatic pressure.

Puttick et al. [44] also conducted experiments on indentation of NaCl. Specimens in the form of {100} rectangular prisms were cleaved from the melt grown crystals. They found that the diamond pyramidal indentation at all loads to be well defined. Scanning electron microscopy examination of the indented surfaces showed a shallow depressed trough parallel to the <100> and pile up along <110>. However, in the case of conical indenters, Puttick et al. [44] reported that cracks initiated in the surface at or close to the indentation and then propagated outward and downward to form an angle wing shape.

Puttick [45] conducted extensive studies in the area of fracture transitions in glass. He observed that transition from brittle to ductile to occur when a certain length parameter attains a critical value given by

$$d_{crtical} \alpha \frac{E\gamma}{Y^2} \tag{3.6}$$

or

$$d_{crtical} \alpha \frac{K_c}{Y^2} \tag{3.7}$$

where E is the Youngs modulus, γ is the fracture surface energy, Y is the yield stress in uniaxial tension and K_c is the critical stress intensity factor.

In addition to the static indentation studies, sliding tests were also conducted on some ceramic materials. For example, Veldkamp et al. [46] studied the effect of a wide range of normal forces on scratching of different ceramics to explore the possibility of a ductile to brittle transition. They reported that at very shallow depths a sharp scratching point in the material produced a fully ductile grooving. Also, with increasing force, they observed that cracks first appeared just behind the scratching point which originated from the grove. This is followed by cracks initiating from the side of the particle and propagate in front of it. Subsequent to this, chipping occurs. Veldkamp et al. commented that during this gradual transition a decreasing specific grinding energy with increasing depth could be anticipated.

The presence of a 'plastic' like layer during the single point grinding/scratching of ceramic materials was reported by Zhang [30]. Working on SiC, Al_2O_3, and SiC, Zhang observed that immediately beneath the indenter there existed a plastically deformed layer of thickness "a" which was related to the depth of cut "A". Also, in the microcracking zone Zhang found a linear relationship between the depth of cut A and the deformed layer "a". Though no theoretical expression was derived for the critical depth at which the transition from the brittle to the ductile regime took place, however, from his experimental data a relation of the type

$$a = \alpha A \tag{3.8}$$

can be developed for the ductile regime, where α is a constant which depends upon the properties of the material.

Researchers at North Carolina State University [4,47] who coined the term of ductile regime grinding base their argument on an hypothesis put forth by Kendall [48]. Kendall argued that plastic deformation is essentially a volume process and therefore must depend on the cube of the characteristic dimension. On the other hand, crack generation and crack propagation are proportional to the area of the crack and hence should depend on the square of the characteristic dimension. As the characteristic dimension gets smaller the amount of energy necessary to initiate plastic deformation process is lesser than that required for crack generation. It, therefore, follows that at a certain critical depth, the plastic deformation process may be energetically favoured to the crack generation process. Using this hypothesis Bifano and Blake [4, 47] conducted grinding as well machining experiments on different brittle materials, including amorphous glasses, advanced ceramics, and semiconductors such as germanium and silicon. Based on their experiments, Bifano [35] postulated that at small depth of cut in grinding required to achieve the ductile regime on a relatively hard material, there is a definite size effect i.e. hardness is not necessarily an invariant material property but rather varies with the depth of cut(doc) - increasing with decreasing doc. For diamond turning, Bifano [35], developed the following expression for the critical depth of cut for germanium and silicon :

$$E_s \alpha \left(\frac{\sigma^2}{E}\right) d^3 \tag{3.9a}$$

where E_s is the elastic strain energy stored in the plastic zone and E is the Youngs modulus. Taking γ as the surface energy required to create new surfaces then, crack energy E_f is given as

$$E_f \alpha \ \gamma d^2, \tag{3.10}$$

But

$$K_c = \sqrt{2\gamma E} \tag{3.11}$$

or

$$\gamma = \frac{K_c^2}{2E} \tag{3.12}$$

$$E_f \ \alpha \left(\frac{K_c^2}{2E}\right) d^2 \tag{3.13}$$

and

$$d = d_{crtical} \ \alpha \ \left(\frac{K_c}{H}\right)^2 \tag{3.14}$$

Special Reference to Glass

Researchers working in the area of machining/grinding of brittle materials and propose support the "ductile" regime grinding concept generally use the data obtained for glass as a basis and apply it to ceramics. However, as is well known, there are a number of differences between ceramics and glass including the following:

(a) glass is an amorphous solid and has no definite crystalline structure like the other ceramics.

(b) glass flows in a manner similar to that of a liquid (viscous) above the glass transition temperature.

(c) glass, as in the case of single crystal material, is structurally a large molecule and contains no internal surfaces, holes or inclusions having the dimensions which approach the wavelength of light.

(d) being amorphous glass may take any structural configurations under the action of stress, which implies that the interatomic distances before and after the application of stress need not be the same.

When subjected to stress, glass behaves in a different manner than those of ductile metals or other brittle materials, such as ceramics. The basic deformation of glass is closely related to the atomic structure. As against the dense packing usually encountered in the case of metals, glass being amorphous, has a certain amount of free volume. The free volume here refers to that fraction of glass which has a lower atomic coordination than that of the reference material. When subjected to stress the loose/weak bonding between the free volume and the surrounding material will result in local rearrangements.

Since glass generally fractures on the application of any appreciable amount of load, indentation hardness tests on this material were not attempted for a long time. Working on borosilicate crown glass and extra dense flint glass, Taylor [49] found some evidence of deformation beneath the moving load. This is interpreted as due to the presence of a large hydrostatic pressure beneath the indenter, as will be shown in in the present investigation using the finite element analysis. Taylor's work is considered as pioneering as he has shown that (i) hardness of glass can be measured and (ii) there is some form of deformation occurring beneath the indenter/moving load. Taylor also found the deformed material to pile up, similar to the phenomena observed with conventional ductile materials. In fact this is one of the reasons he cites for terming the deformation as plastic flow. Though this deformation was termed as "plastic flow" by Taylor, it has been a point of intense debate [29]. Other explanations that have been put forth for the plastic flow or deformation in glass will be discussed in the next section. Taylor's work was closely followed by studies by Ainsworth [50] who found that distribution of flaws and defects

determine the strength to a very large extent. Based on the data of Fisher and Hollomon [50], Ainsworth concluded that the indentation hardness testing should be conducted on a surface area very much lower than 0.1 mm^2. Using the relation H=cY developed by Tabor [51] for the hardness of metals, Ainsworth calculated the yield strength of plate glass to be of the order of ~ 2.0 GPa (with a value of 2.7 for c in the above equation). This value is about 30 times the stress required to break glass. Ainsworth argued that the plastic flow of glass can take place provided the volume of glass involved is small. Ainsworth, in the present writers opinion, was perhaps referring to the the size effect which may be the basis for explaining ductility in brittle materials.

Marsh [52] reported his findings of plastic-like deformation in glass during indentation/scratching. He reported that even at room temperature glass could flow plastically, and that the flow stress is a strong function of the time of loading. Marsh's conclusion of plastic flow in glass was based on the following observations (i) when scratched with diamond, large furrows were produced (ii) diamond indenter when impressed on glass gave impressions which are similar to that on hardened steel. He also argued that glass could not reach the predicted terminal fracture velocities for brittle solids. Marsh observed that the flow stress of glass is generally much lower than the theoretical cohesive strength of the material. Hagan [53] also studied the shear deformation resulting from the indentation of glass. He reported that apart from the initial compaction of the silicate network, flow occurs. Also, a departure from the ideal plastic behavior which requires that the spiral flow lines meet at 90° was not found (the lines were found to meet at 100 °). Hagan attributed this deviation from the ideal rigid-plastic behavior to the initial densification.

Huerata and Malkin [54] conducted multipoint grinding experiments with silicon carbide and diamond abrasives on glass and reported plastic deformation of glass. They observed that the material removal in the case of diamond grinding of glass was a

combination of the chipping and ductile deformation processes. They developed a relationship for the total specific energy during the process as

$$U_{total} = U_{fracture} + U_{\text{ductile deformation}} \tag{3.14}$$

The specific energy for fracture U_f is given by the surface energy for generation of new surfaces per unit volume of material removal. They derived the following expression for estimating the specific energy for fracture.

$$U_f = a\gamma \tag{3.15}$$

where a is the surface area per unit volume and γ is the surface energy of glass. If the surfaces are assumed to be uniform and cubic with a dimension of c, then a in the above expression is equal to 'c'. Substitution of this in 3.13 and 3.14 gives

$$U_f = \frac{6\gamma}{c} \tag{3.16}$$

Based on this expression, U_f was calculated as 3.1 J/mm^3 and this value was found to be about one third of the total specific energy consumed during the process. Hence, they attributed that a significant amount of energy for plastically removing the material.

Single point and multiple point grinding experiments were also conducted by Kirchner [55]. He found cracking in both multipoint and single point grinding of glass. This crack system included tensile cracks formed behind the contact in response to the frictional forces and median cracks /radial cracks formed beneath the contact. Kirchner cautioned that though single point grinding provides a useful simulation of the multipoint there were some salient differences between these two namely- in single point grinding, the

interaction between the neighboring points are not simulated and, the forces on the diamond may be too great and may lead to excessive crushing.

Densification

Following Ainsworth work [50] there were other reports [29, 56] on the measurement of hardness of glass. Though the values reported were about the same, the very measurement of hardness and the underlying physics came under much debate.

In general, dense crystalline compounds subjected to pure hydrostatic pressure retain their original shape. This is, however, under the assumption that no crystal transformation has occurred. However, in the case of certain oxide glasses, subjected to uniaxial compression a change in volume is found [29]. This change in volume is referred to as compaction because of the associated increase in density. Since glass can accommodate changes in the structure under the action of stress, it was pointed out that densification may be taking place during hardness measurement of glass. This opinion received strong support after Bridgman and Simon [27] reported their findings. Under hydrostatic pressures of the order of 10MPa, Bridgman et al. [27] found that the changes in density could be as much as 17.5 %. Following this Peter [29] proposed densification as the most probable mechanism for the deformation of glass. Since density and the refractive index of the material are related by the Lorentz law (the change in refractive index is related to the density of the material by the relation $\rho N_A \alpha = 3M \varepsilon_0 \left[\frac{n^2 - 1}{n^2 + 1}\right]$, where N_A is the Avagadro's number, M is the molecular weight, ρ is the density, α is an atomic parameter and n is the refractive index of the material), Peter measured the change in refractive index to prove the role of increased density as the only possible mechanism during indentation of glass. Ernsberger [56], working along the lines of Peter, also found a change in refractive index by as much as 0.08. Ernsberger went one step further and calculated the depth of deformed zone to be around 1/4 the diameter of the indenter. Based on this finding,

Ernsberger redefined the hardness of glass as the amount of hydrostatic pressure required to produce densification.

Sakka and MacKenzie [57] in a study on the effects of high hydrostatic pressure on glass addressed such questions such as the effect of shear on densification, the possibility of pure hydrostatic pressure alone contributing to the densification and structural changes which accompany densification. Sakka et al [57], based on the data provided by MacKenzie et al., argue that pure hydrostatic pressure alone cannot produce the required densification. To study the effect of shear on densification they used two different sets of pressure transmitting media namely Al_2O_3 and AgCl. Al_2O_3 as a transmitting medium was assumed to have shear associated with it whereas AgCl was assumed to produce pure hydrostatic conditions. They found that, densification with Al_2O_3 was more than that with AgCl, under the same operating pressures. They concluded that densification resulting from the compaction of silica glass in the rigid state depends on the external shear inherent in any pressure transmitting device - i.e more the shear associated with the process, more is the densification and vice versa. The same logic has been extended to explain the 'flow' in glass - as the local hydrostatic pressure can be as high as 1~3 GPa. They argued that since there is bound to be a shear component of stress associated with the indentation process, it is possible that some densification could result.

An important short comings of the densification theory is it could not explain the chips and the chip-like materials that are produced during the scratching process. Ernsberger, acknowledged this fact when analyzing the results of Taylor. More recent experiments by Finnie et al. [58] has shown proof of the fact chips or chip-like structures can be produced during scratching of glass. Finnie, however has not proposed any mechanism responsible for the chip formation.

Based on the findings of Ernsberger [56], Peter et al. [29] and Finnie [58] it may be concluded that the deformation prior to cracking cannot be attributed solely to either

densification or to plastic flow. It is possible that both these mechanisms may be operational.

CHAPTER IV

ANALYTICAL SOLUTION OF THE ELASTO-PLASTIC INDENTATION PROBLEM

The elasticity of the material plays an important part in micro-indentation. Unlike in the case of fully elastic and fully plastic problems which have been well established methods of analysis, the elasto-plastic indentation problem has not yet been fully understood. Analysis of the indentation problem with the elastic strains comparable to the plastic strains was conducted by Samuels and Mulheran [21]. They observed that in some cases, the deformation below the indenter did not show an outward flow of material as predicted by the plasticity theory, but resembled radial flow type compression of material. This phenomenon was subsequently analyzed by Marsh [52] who equated the deformation beneath the indenter to that of an expanding sphere. This representation of the indentation process, assumes that the contact surface of the indenter is encased in a hemispherical core of radius a, (equals to 0.5d), where d is the diagonal of the indenter. Within this core, the deformed material is assumed to exert a hydrostatic pressure p. In such a case, the plastic zones are small and the magnitude of the elastic and plastic strains are almost the same. Consequently, the material that is displaced by the indenter can be accommodated by the elastic expansion of the surrounding material. This compression model, which is mathematically represented by an expanding sphere is characterized by the following features [18] :

* the contact or the indentation with the surface produces radial compression of the

hemispherical shells. For the purpose of analysis it is assumed that all these shells are centered about the point of contact. The strains immediately adjacent to the indenter are large and decrease progressively towards bulk of the material. Regions of higher strains are assumed to occur very near the tip of the indenter.

* Unlike in the case of cutting mechanism, the indented surface is formed by the original test surface folding progressively about the axis of the indenter. Because of this, the surface remains almost unaltered except for a downward dent like formation just at the point of indentation. The additional surface area required for this downward stretching at the point of indentation is produced either by stretching the original source or by the cutting of material. As to which of these two mechanisms will be operational in the process depends on the yield strength of the material i.e lesser the yield strength, greater the chance for stretching or vice versa.

The compression type mechanism is reported to depend on some material properties [10]. For example, in the case of annealed metals, when the indenter sinks into the metal the material adjacent to the indenter becomes workhardened in comparison with the material away from it [10]. As the indenter begins to sink further, it will take the workhardened material along with it. The net effect is that workhardened metal and the indenter together will act as one indenter. This will lead to the depression of the material immediately adjacent to the indenter.

This type of mechanism is also found to be operational in the case of materials which have a low E/Y value. Table 4.1 shows the E/Y and P/Y (H_V/Y) values for some brittle materials such as ceramics and diamond. Working on glass, Marsh [52], observed that in the case of materials which have a low E/Y value, the compression type mechanism is operational. He also found that the basic form of usual method of representation of hardness of the form $\frac{H_V}{Y} = 3$ to be invalid. He suggested that in the case when E/Y is low,

the relationship between the hardness and the yield strength is expressed by more complicated forms which also involves the Youngs modulus (E) of the material. It should be noted that for materials with low Young's modulus to yield strength ratio, the value of hardness to yield is generally more than 3.0 (see Table 4.1). The unusually high value in the case of diamond may probably due to its unique crystal structure.

TABLE 4.1

E/Y VALUES OF SOME BRITTLE MATERIALS

Material	E (GPa)	Y (MPa)	H_V (GPa)	E/Y	H_V/Y
Al_2O_3	380	6362	23.18	59.72	3.644
BeO	311	3519	11.15	88.37	3.17
MgO	207	1959.6	6.42	105.63	3.28
SiO_2	69	1856	5.38	37.125	2.89
Diamond	1035	8901	95.08	116.26	10.88

Hill's Spherical Cavity Solution

As mentioned in the introductory part of this chapter, when the elastic strains are comparable with those of the plastic, the analytical modelling of the indentation problem becomes difficult. In such cases, it may be necessary to use certain indirect methods of analysis. One such approach is to assume that the subsurface displacements produced by an indenter are approximately radial from the point of contact. The deformation in the localized

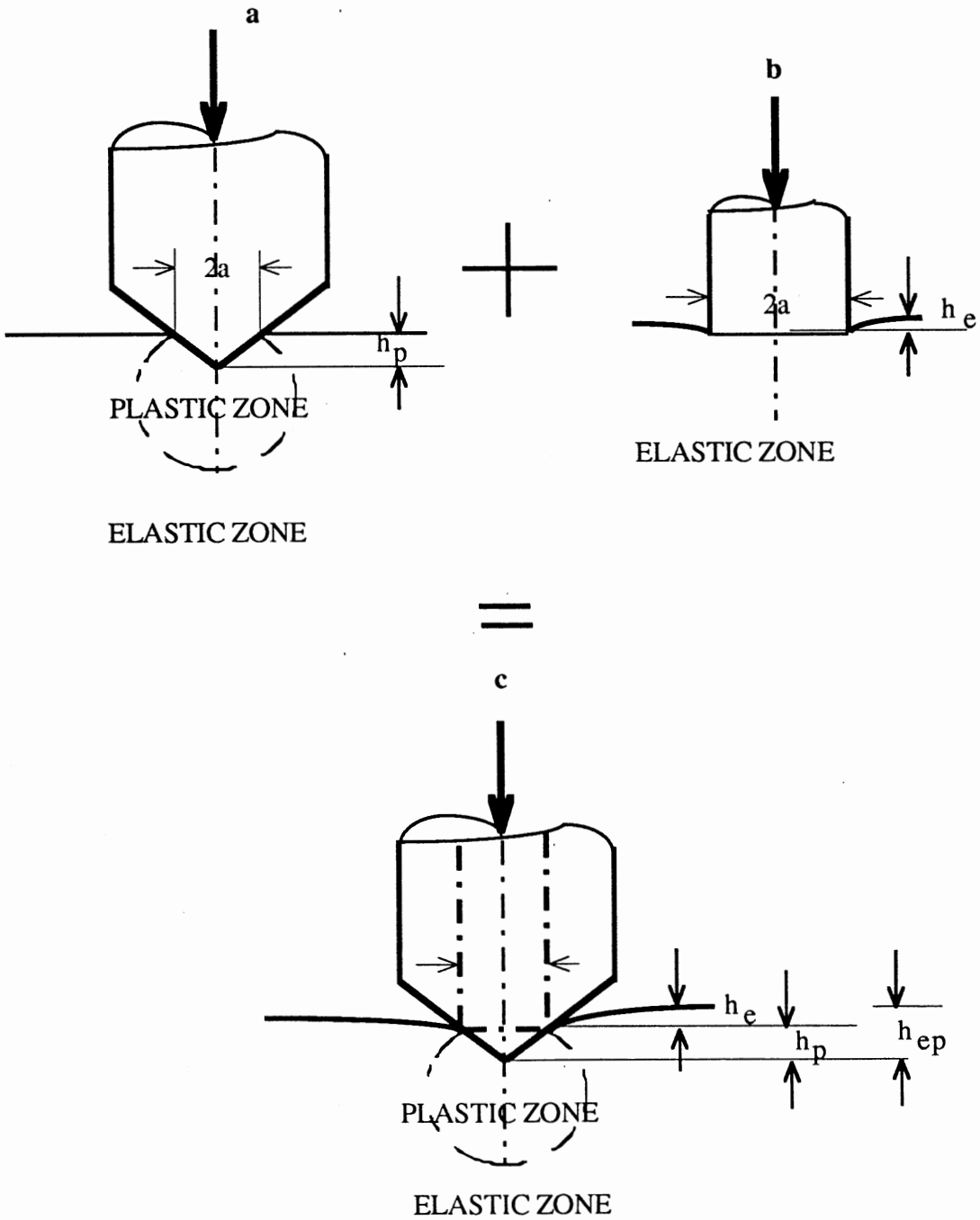

Figure 4.1 Elasto - Plastic Solution of the Indentation Problem [59]

region just beneath the indenter is modelled as a (hemi)sphere which is expanding under uniform internal pressure. The solution to this problem was first developed by Marsh [52]. In this section, details of that analysis will be presented. This solution was first given by Hill [60].

Calculation of Stresses

The state of stress in a sphere subjected to an internal pressure is given in the general form as [31]

$$\sigma_r = \frac{C}{R^3} + D \tag{4.1}$$

where C and D are constants. If a and b are taken as the internal and the external diameters of the sphere subjected to an internal pressure of p_i and an external pressure of p_o, then

$$- p_i = \frac{C}{a^3} + D \tag{4.2}$$

$$- p_o = \frac{C}{b^3} + D \tag{4.3}$$

Solving for C and D and substituting in (4.1) we get for the radial stress σ_r

$$\sigma_r = \frac{p_o b^3 (R^3 - a^3)}{R^3 (a^3 - b^3)} + \frac{p_i a^3 (b^3 - R^3)}{R^3 (a^3 - b^3)} \tag{4.4}$$

The tangential stress σ_t can be obtained by considering the equilibrium of the elemental section as shown in Figure 4.2.

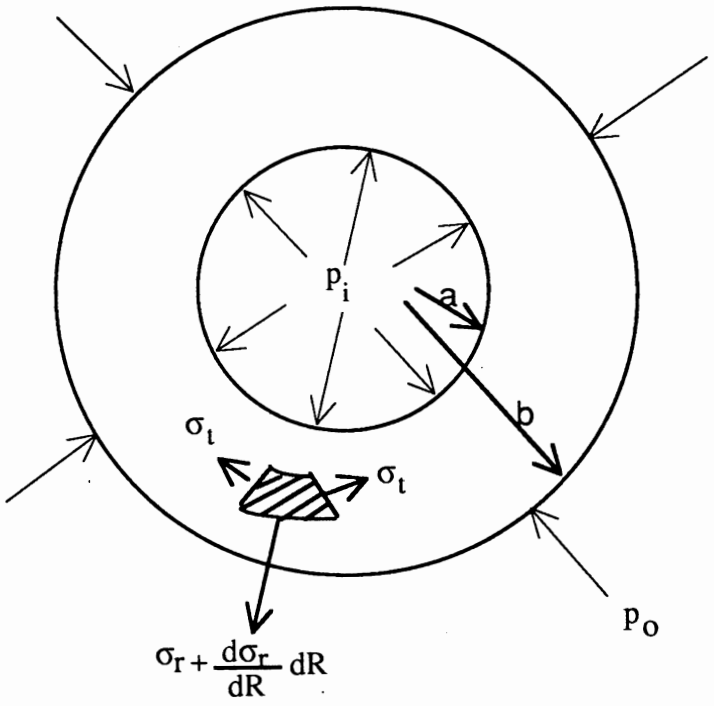

Figure 4.2 Stress Diagram for a Spherical Element

and substituting for σ_t and σ_r from equation (4.9) we get

$$Y = \frac{-3p\, a_o^3}{2r^3\left[\left(\frac{a_o}{b_o}\right)^3 - 1\right]} \tag{4.11}$$

But, yield begins at the inner surface when $r=a_0$. Therefore

$$Y = \frac{-3p}{2\left[\left(\frac{a_o}{b_o}\right)^3 - 1\right]} \tag{4.12}$$

With increasing internal pressure, the plastic zone increases in dimension. Due to symmetry, the plastic zone is assumed to be spherical. If c denotes the radius at any instant, then in the elastic region the radial and tangential stresses (σ_r, and σ_t) are given as

$$\sigma_r = -A\left[\left(\frac{b_o}{r}\right)^3 - 1\right] \tag{4.13}$$

$$\sigma_t = A\left[\frac{b_o^3}{2r^3} + 1\right] \tag{4.14}$$

where A is any constant.

At the boundary r= c, we have yielding. Application of Tresca's yield criterion, gives

$$A = \frac{2Yc^3}{3b_o^3} \tag{4.15}$$

Substituting (4.15) in (4.13) and (4.14), we get

$$\sigma_r = -\frac{2Yc^3}{3b_0^3}\left[\frac{b_0^3}{r^3} - 1\right] \tag{4.16}$$

and

$$\sigma_t = \sigma_\theta = \frac{2Yc^3}{3\,b_0^3}\left[\frac{b_0^3}{2\,r^3} + 1\right] \tag{4.17}$$

In the plastic zone we have

$$\frac{\partial \sigma_r}{\partial r} = \frac{2\,(\sigma_\theta - \sigma_r)}{r} \tag{4.18}$$

Integrating equation (4.18), we get

$$\sigma_r = 2Y \log (r) + B \tag{4.19}$$

But from equation (4.12) we have $p = \frac{2Y}{3}\left[1 - \left(\frac{a_o}{b_o}\right)^3\right]$. Also, since σr must be continuous across the plastic boundary, we have

$$\sigma_r = \frac{2Y}{3}\left[1 - \left(\frac{c}{b_o}\right)^3\right] \tag{4.20}$$

This condition is obtained by taking $P = -\sigma_r$. at a=c

On equating (4.19) and (4.20), we get

$$B = -\,2Y \log (c) - \frac{2Y}{3}\left[1 - \left(\frac{c}{b_o}\right)^3\right] \tag{4.21}$$

Hence

$$\sigma_r = -\,2Y \log\left(\frac{c}{r}\right) - \frac{2Y}{3}\left[1 - \left(\frac{c}{b_o}\right)^3\right] \tag{4.22}$$

and from equation (4.10)

$$\sigma_\theta = Y - 2Y \log\left(\frac{c}{r}\right) - \frac{2Y}{3}\left[1-\left(\frac{c}{b_o}\right)^3\right] \tag{4.23}$$

From which the pressure P can be calculated by substituting $P = -\sigma_r$

$$P = 2Y \log\left(\frac{c}{a}\right) + \frac{2Y}{3}\left[1-\left(\frac{c}{b_o}\right)^3\right] \tag{4.24}$$

Calculation of Strains

In order to correlate the stresses developed in the spherical cavity with those in the indentation it is necessary to calculate the strains produced. In this section, strains are computed based on Hill's formulation [60]. In order to compute the displacements of the individual elements, Hill suggested that it is convenient to take the movement of the plastic boundary as the indication of the progress of the deformation process.

Consider a particle in the plastic portion moving with a velocity v. If the plastic boundary moves through an elemental distance dc, then the displacement of the particle can be written as

$$du = \frac{\partial u}{\partial c} dc + \frac{\partial u}{\partial r} dr \tag{4.25}$$

or

$$du = \left[\frac{\partial u}{\partial c} + v\frac{\partial u}{\partial r}\right] dc$$

$$= \frac{\left(\frac{\partial u}{\partial c}\right)}{1 - \left(\frac{\partial u}{\partial r}\right)} \tag{4.26}$$

Using the compressibility equation, we get

$$d\varepsilon_r + d\varepsilon_\theta + d\varepsilon_\phi = \frac{1-2\nu}{E}\left(d\sigma_r + d\sigma_\theta + d\sigma_\phi\right) \tag{4.27}$$

But in terms of displacement of the particle, the strains may be expressed as

$$d\varepsilon_r = \frac{\partial}{\partial r}(du) \quad d\varepsilon_\theta = d\varepsilon_\phi = \frac{du}{dr} \tag{4.28}$$

Also, stresses $d\sigma_r$ and $d\sigma_\theta$ can be expressed as

$$d\sigma_r = \left[\frac{\partial \sigma_r}{\partial \sigma_c} + \nu \frac{\partial \sigma_r}{\partial r}\right] dc \tag{4.29}$$

and

$$d\sigma_\theta = d\sigma_\phi = \left[\frac{\partial \sigma_\theta}{\partial \sigma_c} + \nu \frac{\partial \sigma_\theta}{\partial r}\right] dc \tag{4.30}$$

Substituting the above in equation (4.27), we get

$$\frac{\partial v}{\partial r} dc + 2\frac{\nu dc}{r} = \left(\frac{1-2\nu}{E}\right)\left(\frac{\partial \sigma_r}{\partial c} + \nu \frac{\partial \sigma_r}{\partial r} + 2\frac{\partial \sigma_\theta}{\partial r} + 2\nu \frac{\partial \sigma_\theta}{\partial c}\right) dc \tag{4.31}$$

$$\frac{\partial v}{\partial r} + 2\frac{v}{r} = \left(\frac{1-2\nu}{E}\right)\left(\frac{\partial}{\partial c} + \nu \frac{\partial}{\partial r} + \right)\left(\sigma_r + 2\sigma_\theta\right) \tag{4.32}$$

Substituting the expressions for σ_r and σ_t from equations (4.17) and (4.18) in equations (4.31,4.32) we get

$$\frac{\partial v}{\partial r} + 2\frac{v}{r} = 6Y\left(\frac{1-2\nu}{E}\right)\left[\frac{v}{r} - \frac{1}{c}\left(1 - \frac{c^3}{b_0^3}\right)\right] \tag{4.33}$$

Solving the above partial differential equation (4.33), we get

$$v = 3\frac{(1-\nu)Yc^2}{Er^2} - \frac{2(1-2\nu)Y}{E}\left(1 - \frac{c^3}{b_0^3}\right)\frac{r}{c} \tag{4.34}$$

Since v=da/dc at r=a

$$\frac{da}{dc} = 3\frac{(1-\nu)Yc^2}{Er^2} - \frac{2(1-2\nu)Y}{E}\left(1 - \frac{c^3}{b_0^3}\right)\frac{a}{c} \tag{4.35}$$

Correlating Hill's Solution with Indentation Parameters

In this section the indentation parameters such as the indenter geometry and the depth of indentation are correlated with the state of stress obtained in the previous section. The methodology developed by Johnson [61] will be presented. Johnson in his analysis made the following assumptions :

* the hydrostatic pressure in the core is equal to the radial component of stress in the external zone at r=a.
* the volume of material displaced by the indenter is equal to the increase in the volume of the core.

Consider equation (4.24) when the cylinder is expanding from a zero initial radius, we have

$$P = 2Y\log\left(\frac{c}{a}\right) + \frac{2Y}{3} \tag{4.36}$$

Also from equation (4.35) the radial displacement of the particle is given by da/dc=du/dc or

$$\frac{d(u)}{dc} = 3\frac{(1-\nu)Yc^2}{Er^2} - \frac{2(1-2\nu)Y}{E}\left(1 - \frac{c^3}{b_0^3}\right)\frac{a}{c} \tag{4.37}$$

Assuming that the increase in volume of the core is equal to the volume of the material displaced by the indenter, we get

$$\frac{2}{3}\pi a^2 da\,(u) = \frac{1}{3}\pi a^2 dh \tag{4.38}$$

But from the geometry of indentation (see Figure 4.3) $\tan\beta = \frac{dh}{da}$ we get

$$\frac{1}{2}\tan\beta\, da = du(a) \tag{4.39}$$

$$\frac{du(a)}{dc} = \frac{3(1-\nu)Y c^2}{E r^2} - \frac{2(1-2\nu)Yr}{E c} \tag{4.40}$$

$$\frac{1}{2}\tan\beta\frac{da}{dc} = \frac{3(1-\eta)Y c^2}{E r^2} - \frac{2(1-2\eta)Yr}{E c} \tag{4.41}$$

Using the conditions of geometrical symmetry, we have da/dc = a/c, which on substitution in equation (4.41)gives

$$\frac{E}{Y}\tan\beta = 6(1-\eta)\left(\frac{c}{a}\right)^3 - 4(1-2\eta) \tag{4.42}$$

when ν=0.5 we have

$$\frac{c}{a} = \left[\frac{E}{Y}\tan\beta\right]^{1/3} \tag{4.43}$$

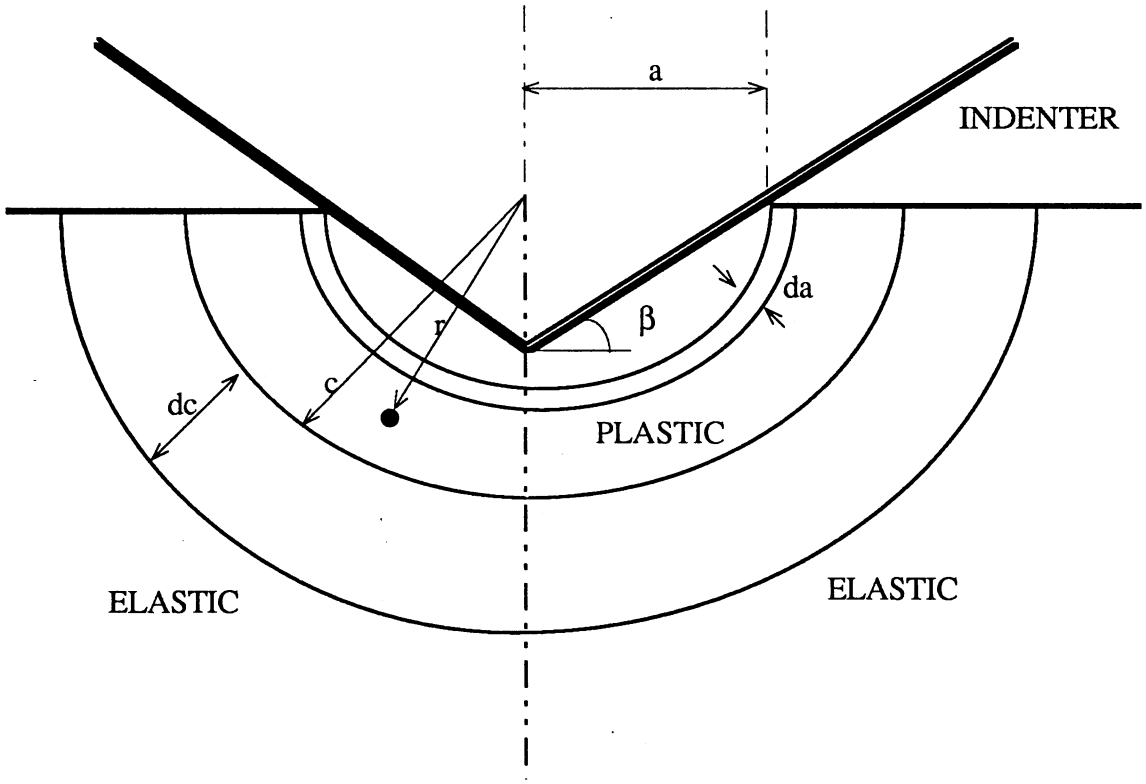

Figure 4.3 Johnson's Model for Correlating Indentation Parameters with Hill's Spherical Cavity Solution [61]

which on substitution in (4.36) gives

$$\frac{P}{Y} = \frac{2}{3}\left[1 + \log\left(\frac{1}{3}\frac{E}{Y}\tan\beta\right)\right] \tag{4.44}$$

It may be noted that the Hill's solution is for a *complete sphere*, where as in the case of indentation a *hemisphere* expands under internal pressure. Also, in the indentation problem, one has to take into account the free surface. Hence, in applying this solution for the indentation problem, it has to be modified so that these factors are considered. This modification was done by Chiang et al. [62] who used the procedure developed by Mindlin [63] to arrive at a free surface boundary condition for an expanding hemisphere. One of the salient features of Chiang's analysis is the ability to take into consideration the various cracking sequences during the indentation process in brittle materials.

CHAPTER V

MODIFIED HILL'S SPHERICAL CAVITY SOLUTION FOR INDENTATION OF BRITTLE MATERIALS

Bridgman's pioneering work [27, 64, 65] has established that in order to induce plasticity in brittle materials, such as glass, alumina and marble the state of stress should be such that there is a considerable amount of superimposed hydrostatic pressure (of the order of few tens of mega pascals). The effect of extremely high hydrostatic pressure on the response of materials is two fold [66]

(a) from a continuum mechanics point of view, high hydrostatic pressure will result in the displacement of the intrinsic or the Mohr's curve.

(b) from a microscopic view the effect of high compressive pressure will be to close the microcraks as they are formed.

A lucid explanation of the effect of high hydrostatic pressures on the behavior of materials, in terms of the stress-strain behavior, was put forth by Pugh [67]. He argued that though the stress-strain curve is a representation of the basic material property, fracture itself was determined by the absolute value of the tensile strain. Thus, during a uniaxial tensile testing of a specimen under high hydrostatic pressure, a much larger tensile stress is required to cause fracture because of the added compressive stress imposed by the high hydrostatic pressure. With reference to Figure 5.1, the material may fracture at point A when subjected to uniaxial tension, under atmospheric conditions. In contrast, when the same test is carried out under hydrostatic pressure, compressive stresses are imposed and the tensile

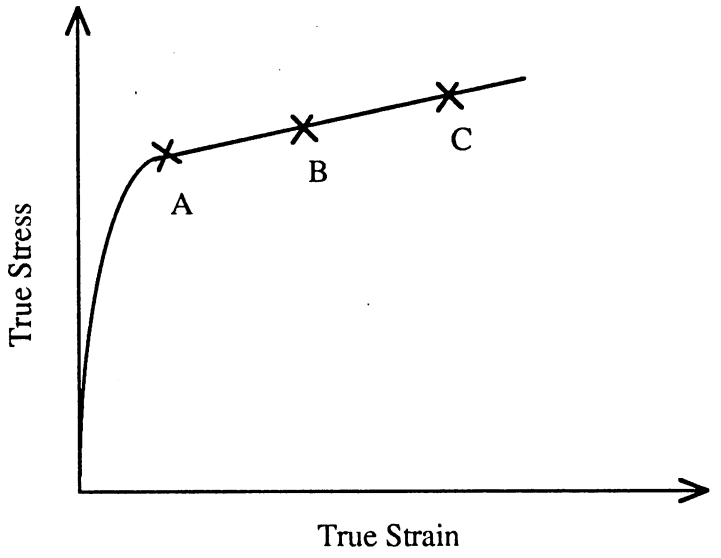

(a) Material with higher workhardening coefficient

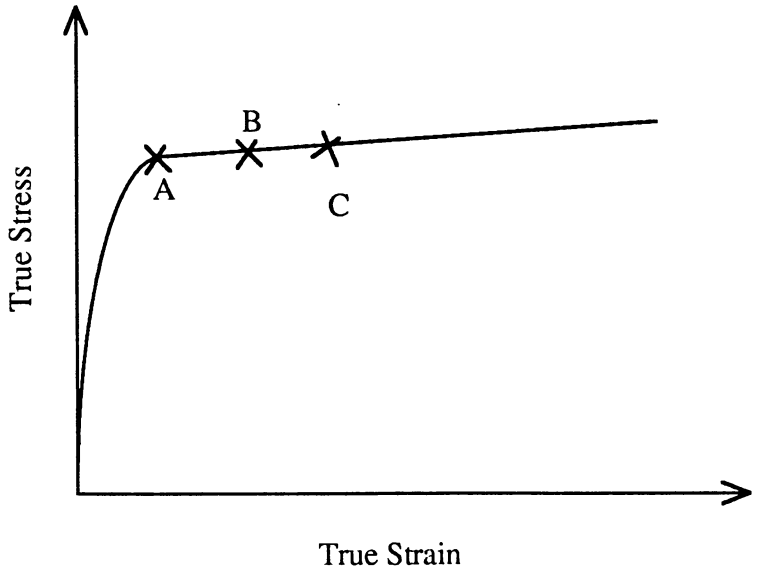

(b) Material with lower workhardening coefficient

Figure 5.1 Effect of Hydrostatic Pressure on Stress-Strain Curve

stress required to cause fracture raises up to point B. Pugh suggested that at still high pressure, fracture is delayed up to point C. In the case of materials having a flatter stress strain curve [Figure 4.1b], only small changes in the hydrostatic pressure are required to shift the point of fracture from B to C.

During the process of indentation also, pressures in the range of 1 ~ 3.0 GPa (the value depends on the yield strength of the material) are usually observed in localized regions [37]. It, therefore, becomes necessary that the effect of hydrostatic pressure be considered when the equations for the stress state are derived.

Yield Criterion

Yield criterion may be defined as any general condition which must be satisfied if yield is to occur. An yield criterion for metals is proposed under the following assumptions - (i) the material is homogeneous and isotropic, (ii) there is no Baushinger effect, and (iii) the hydrostatic component of stress alone does not contribute to yielding. Under these assumptions

$$f(II_{\Sigma D}, III_{\Sigma D}) - Y = 0 \tag{5.1}$$

The last assumption i.e. the hydrostatic component of stress alone does not produce any yielding, is made because the material is taken to be incompressible. Based on these assumptions von Mises proposed that yielding in a material will occur when the elastic energy of distortion reaches a critical value i.e.

$$-II_{\Sigma D} = C_Y \tag{5.2a}$$

which can also be written as

$$(\sigma_1 - \sigma_2)^2 + (\sigma_2 - \sigma_3)^2 + (\sigma_3 - \sigma_1)^2 = 6k^2 \tag{5.2b}$$

where k is the yield stress of the material in pure shear. Tresca proposed that yielding would occur when the resolved shear stress on any plane reaches a critical value.

$$\sigma_1 - \sigma_3 = 2k \tag{5.3}$$

Though in most cases the above stated three assumptions are valid, there are some instances where the material is not homogeneous or dense and hence some of these assumptions no longer hold good. For example, in the case of compression of porous materials (with porosity as high as 40%) it becomes obvious that the hydrostatic stress does produce some yielding. In such cases it becomes necessary that the first invariant of the stress has to be considered. Taking the first invariant of the stress into consideration the yield criterion then becomes

$$f(I_{\Sigma D}, II_{\Sigma D}, III_{\Sigma D}) - Y = 0 \tag{5.4}$$

As stated earlier, in the case of indentation, the localized pressure can reach as much as 1~3 GPa, and this can be partly responsible for the yielding of the material. The problem, therefore would require that the yield criterion for the material (ceramic) be modified so as to take the first invariant of stress into consideration. The principle work in this area (i.e porous materials which yield under hydrostatic pressure) was first reported by Drucker and Prager [68]. Their work was mainly intended for soils and similar materials. They assumed a yield function of the type

$$\sqrt{\alpha J_1^2 + J_2'} = k \tag{5.5}$$

When α is equal to zero this criterion reduces to the Mises condition. When the above equation is represented on the (π) plane (or the principal stress space) it takes the form of a right circular cylinder for $\alpha=0$ and a right circular cone for $\alpha>0$.

Important feature of the above yield criterion can be obtained by considering the plastic potential

$$\varepsilon_{ij} = \lambda \frac{\partial f}{\partial \sigma_{ij}} \tag{5.6}$$

On simplifying the above equation, we have

$$\varepsilon_{ii} = 3\alpha\lambda \tag{5.7}$$

which is known as the cubical dilation. This indicates that the plastic deformation process must be accompanied by an increase in volume.

Green [69] proposed a new yield criterion for materials which showed some amount of deformation when subjected to a certain hydrostatic stress. Arguing that the previous theories were based on the fact that the yield surfaces were unbounded in compression and allowed for little or no strength in tension, Green postulated a yield criterion of the form of

$$f\left(J_1, J_2', v\right) = Y^2 \tag{5.8}$$

where v is the void ratio or the ratio of the solid material to the total volume of voids. Neglecting any interrelation between J_1 and J_2, the above yield criterion may be rewritten as

$$J_2' + \alpha J_1^2 = \delta Y^2 \tag{5.9}$$

where α and δ are functions of v. It can be seen that for $\delta=1$, this yield criterion reduces to the Drucker-Prager model and for $\alpha=0$ and $\delta=1$ to Mises yield criterion. In terms of void ratio, Green calculated the values of the above two constants as

$$\alpha = 1/4 \left[\frac{3\left(1- v^{1/3}\right)}{\left(3 -2v^{1/4}\right)\log v}\right]^2$$

$$\delta = \left[\frac{3\left(1- v^{1/3}\right)}{\left(3 -2v^{1/4}\right)}\right]^2 \tag{5.10}$$

Several other yield criteria considering the first invariant of the stress, have been proposed [70]. But many of them have drawbacks, namely, the constants involved are difficult to evaluate in actual applications.

Hill's Solution with a Modified Yield Criterion

Since the present problem is one in which the hydrostatic stress is very significant, it appears that the problem of indentation of brittle materials be viewed with a yield criterion along the lines those discussed above. Chen [71] carried out an analysis of the indentation of Zirconia ceramic using the spherical cavity solution and a yield criterion of the form of

$$Y = Y_0 + \alpha P \tag{5.11}$$

where Y_0 is the compressive yield stress at zero pressure and P is the hydrostatic pressure or the triaxial confining pressure. Using this criterion, Chen found the stresses in indentation using the spherical cavity solution. We assume a yield criterion of the form of

$$Y = \alpha J_1 + \beta J_2^{1/2} \tag{5.12}$$

It can be seen that this yield criterion is different from that assumed by Chen [71]. Here, it is assumed that the effect of shear stress on yielding, during the indentation process, is not independent of the hydrostatic pressure. Consequently α and β in the equation 5.12, may both vary so as to effect the yield. As stated earlier, if α=0 and β =1 in the above equation, we have the Mises yield criterion. Now, starting with equation (4.11), the yield in the material is given by (Tresca's criterion)

$$\sigma_t - \sigma_r = Y \tag{5.13}$$

where

$$\sigma_r = \frac{p_i a_0^3 (b_0^3 - r^3)}{r^3 (a_0^3 - b_0^3)}$$

$$\sigma_t = \frac{p\left[\frac{b_0^3}{2r^3} + 1\right]}{\left[\frac{b_0^3}{a_0^3} - 1\right]} \tag{5.14}$$

Since, within the spherical cavity the state of stress is everywhere hydrostatic tension [60] we have

$$\sigma_t - \sigma_r = \beta Y_0 - \alpha \sigma_t$$

$$= \beta Y_0 - \alpha \left[\frac{p_i a_0^3 (b_0^3 + 2R^3)}{2r^3 (a_0^3 - b_0^3)}\right] \tag{5.15}$$

which on simplification gives

$$P_0 = \frac{\beta Y_0 \left(b_0^3 - a_0^3\right)}{\frac{3}{2} b_0^{\,3} + \alpha\left(1 + \frac{b_0^3}{2r_0^3}\right)} \tag{5.16}$$

where P_0 is the pressure corresponding to p at r=a. It can be observed that when β=1 and α =0, the above equation reduces to

$$P_0 = \frac{2\, Y_0 \left(b_0^3 - a_0^3\right)}{3 b_0^3} \tag{5.17}$$

which is the same as equation (4.12) of Hill's analysis.

In the plastic portion, the equilibrium equation is given as

$$\frac{\partial \sigma_r}{\partial r} = 2\left(\frac{\beta Y_0 - \alpha \sigma_t}{r}\right) \tag{5.18}$$

and substituting equation (5.13) in (5.18) we get

$$\frac{\partial \sigma_r}{\partial r} = 2\frac{(Y - \alpha\sigma_t)}{r} \tag{5.19}$$

On substituting the value of σ_t from equation (5.14) and simplifying we get

$$\frac{\partial \sigma_r}{\partial r} = 2\frac{\left(\beta Y_0 - \alpha \frac{p_i a_0^3 \left(b_0^3 + 2r^3\right)}{2r^3\left(a_0^3 - b_0^3\right)}\right)}{r} \tag{5.20}$$

Integrating the above equation (5.20),we get

$$\sigma_r = 2\beta Y_0 \log(r) - \frac{\alpha p\, a_0^3}{(a_0^3 - b_0^3)}\left(\log(r) - \frac{b_0^3}{6\, r^3}\right) + C \qquad (5.21)$$

where C is a constant which can be evaluated by imposing the boundary condition, namely at $r=a_0=c$, $p=-\sigma_r$, then (note $p=p_i$)

$$C = -2\beta Y \log(c) \; - \frac{\alpha P c^3}{\left[c^3 - b_0^3\right]}\left\{ - \frac{b_0^3}{6c^3} + \log(c)\right\} - \frac{\beta Y_0 \left(b_0^3 - a_0^3\right)}{\frac{3}{2} b_0^{\,3} + \alpha\left(1 + \frac{b_0^3}{2r_0^3}\right)} \qquad (5.22)$$

Hence,

$$\sigma_r = 2\beta Y_0 \log(r) - \frac{\alpha P a_0^3}{a_0^3 - b_0^3}\left(\log(r) - \frac{b_0^3}{6r^3}\right) + \frac{\alpha P c^3}{c^3 - b_0^3}\left(\log(c) - \frac{b_0^3}{6c^3}\right) -$$

$$\beta Y_0 \frac{\left(b_0^3 - c^3\right)}{\frac{3}{2} b_0^3 + \alpha\left(1 + \frac{b_0^3}{c^3}\right)} - 2\,\beta Y_0 \log(c) \qquad (5.23)$$

from the above equation when $\alpha=0$, $\beta=1$, we have

$$\sigma_r = -2Y \log\left(\frac{c}{r}\right) - \frac{2Y\left(b_0^3 - c^3\right)}{3b_0^3} \qquad (5.24)$$

which is the same as equation.(4.22) in Hill's formulation. Using equation 5.15, the tangential stress is given as

$$\sigma_t = \frac{1}{\alpha + 1}\left[\beta Y_0 + 2\beta Y_0 \log(r) - \frac{\alpha P a_0^3}{a_0^3 - b_0^3}\left(\log(r) - \frac{b_0^3}{6r^3}\right) + \frac{\alpha P c^3}{c^3 - b_0^3}\left(\log(c) - \frac{b_0^3}{6c^3}\right) - \beta Y_0 \frac{(b_0^3 - c^3)}{\frac{3}{2}b_0^3 + \alpha\left(1 + \frac{b_0^3}{c^3}\right)} - 2\beta Y \log(c)\right] \quad (5.25)$$

These equations, which take into consideration the effect of hydrostatic pressure, may be used to define the state of stress in the case of indentation of brittle materials. In Chapter VI it will be shown that large hydrostatic pressures are produced in the regions just below the point of indentation. Also, the hydrostatic pressure is related to the E/Y of the material, i.e. the lower the E/Y value higher is the hydrostatic pressure and vice versa. Since brittle materials, such as advanced ceramics have generally low E/Y value, it is suggested that the above equations may be used to determine the stresses in the indentation process, using the Hill's spherical cavity solution. The effect of considering the hydrostatic stress is two fold : in the case of materials, such as glass, where the structure can accommodate microscopic alterations (without macroscopic changes), densification may occur . In the case of other brittle materials which are fully dense such as alumina, silicon nitride, the effect would be to suppress the formation of cracks and thus allow for some amount of plastic deformation.

CHAPTER VI

FINITE ELEMENT ANALYSIS OF INDENTATION

Finite element methods were developed in the early 70's to analyze complex physical phenomenon. It has since been widely used for varied engineering applications. Hardy [15] was among the first to use FEM for analyzing the elasto-plastic indentation process. He studied the Hertzian indentation of ductile materials, such as steel. Yausi and Imoka [72] were among the early investigators to carry out FEM studies on elasto-plastic indentation of brittle materials. Similar analysis has been carried out following that work by others, for example, Franse [73]. A similarity between the analysis of Yausi et al. [72], Franse, and the present investigation is that in all these cases glass has been modelled as an elasto-plastic solid with no cracks.

Formulation

The finite element analysis of the indentation was carried out using the commercially available ABAQUS FEM package. To study the deformation at small depths of indentation, the elasto- plastic option of ABAQUS is made use of. The elasto-plastic formulation is based on the Prandtl-Reuss flow rule. The incremental flow stress is a function of the total strain. Plastic deformation takes place when the stress is beyond the elastic limit. The total incremental strain $d\varepsilon$ can therefore be expressed as

$$\{d\varepsilon\} = \{d\varepsilon^{el}\} + \{d\varepsilon^{pl}\} \tag{6.1}$$

where $d\varepsilon^{el}$ and $d\varepsilon^{pl}$ are the incremental elastic and plastic components of the strain. In the above, the elastic part of the response is assumed to be derivable from an elastic strain energy density potential so that the stress is defined as

$$\sigma = \frac{\partial U}{\partial \varepsilon^{el}} \tag{6.2}$$

where U is the strain energy density potential. The inelastic part of the deformation is defined by the flow rule which is written as

$$d\varepsilon^{pl} = d\lambda \frac{\partial g}{\partial \sigma} \tag{6.3}$$

where g is the flow potential. Similarly, the deformation F can also be broken into

$$F = F^{el} + F^{pl} \tag{6.4}$$

The yield criterion, in the plastic region is expressed in the form

$$\overline{\sigma} = \sqrt{\frac{3}{2} \sigma'_{ij} \sigma'_{ij}} \tag{6.5}$$

The rigid body subjected to indentation and undergoing deformation was modelled using 1250 continuum axisymmetric elements (CAX4). The indenter itself was modelled using the RIGID SURFACE option in ABAQUS. This option ensures that the indenter itself does not undergo any deformation. The initial mesh along with the indenter is shown in Figure 6.1

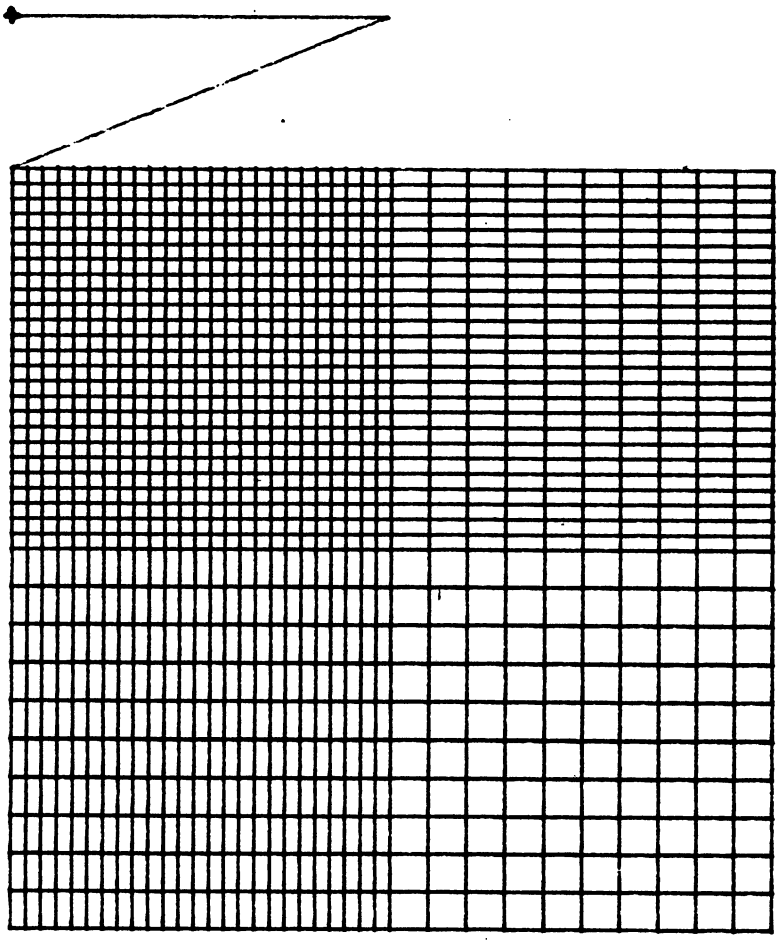

Figure 6.1 Finite Element Mesh used for the Indentation problem

Two different shapes of indenters were used during analysis - conical with 90° and 136° included angles. A major problem in the convergence of the solution, was the die penetration problem. This problem was over come by prescribing some width (0.125μm) at the bottom of the indenter, as against the point shape previously mentioned. It should be noted that the angles mentioned are those in without considering the small "land" at the bottom of the indenter.

Figure 6.2, shows the direction of flow of material in glass at a indentation depth of 10μm depth in glass. From the direction of flow, it is evident that beneath the indenter the material flows in a radial direction, as assumed in the formulation of the elasto-plastic indentation problem in Chapters IV and V. Hence, it can be seen that the the application of Hill's spherical cavity solution is valid. Figure 6.3 shows the hydrostatic stress contours, at 10μm indentation in glass. From this figure it can be observed that the maximum hydrostatic stress of around 3.2 GPa occurs just below the indenter and decreases with increase in distance from the tip of the indenter.

Figures 6.4 show the variation in the maximum principal stress along the axis of symmetry in indentation, at various depths in indentation of glass β=45° Figure 6.5 and 6.6 shows a similar variation for β=45°. The variation in the maximum principal stress along the axis of symmetry for various ductile materials is shown in Figure 6.7. From all these graphs it can be observed that the maximum principal stress is highly compressive just below the indentation, it becomes tensile with increasing distance,and finally saturates to a zero value at some distance away from the tip of the indenter. However, a small variation of the above stated can be seen in the indentation of glass at 5μm depth [Figure 6.6]. In this case the stress state is tensile below the point of indentation i.e it never registers a compressive value.

Figure. 6.8 is shown the variation in the maximum principal stress obtained by Franse [73] in the indentation of glass. Making use of Equation 4.44, with E=90 GPa,

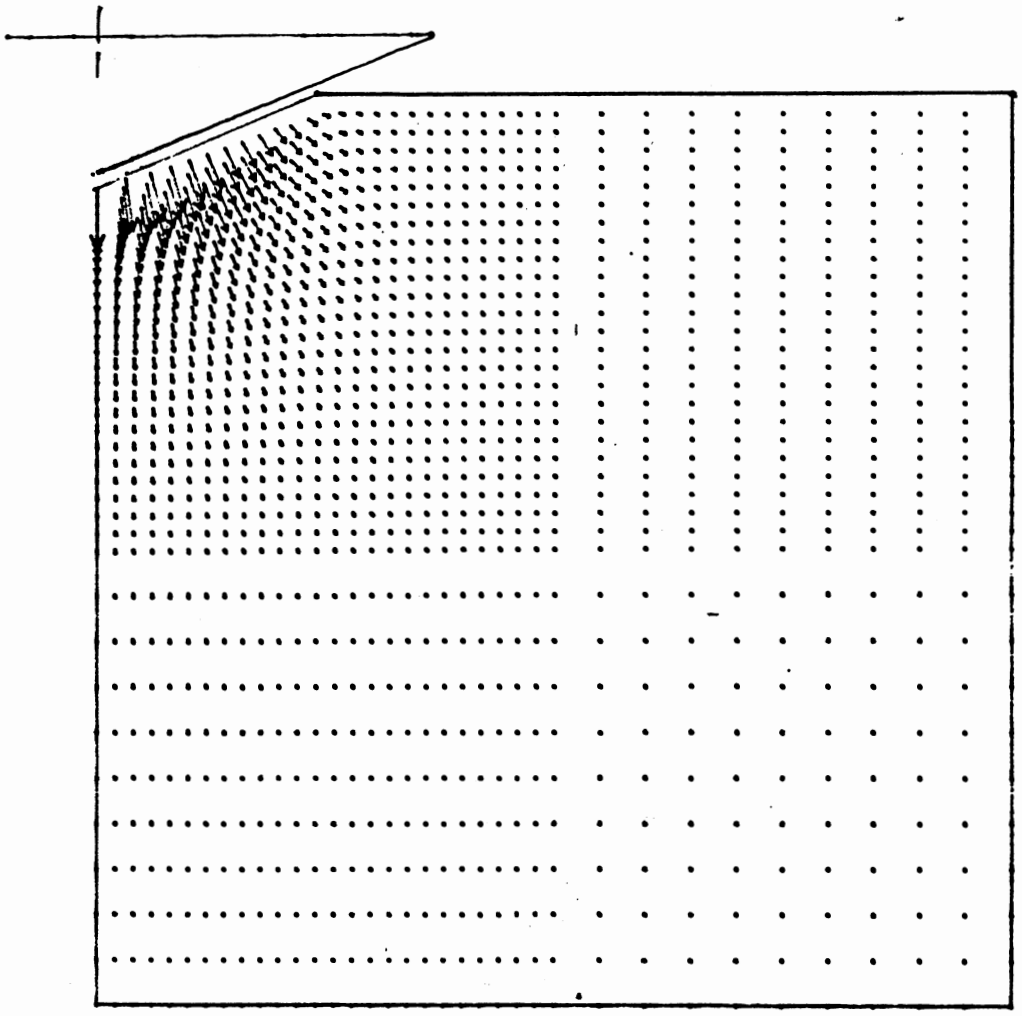

Figure 6.2 Direction of Material Flow in Indentation of Glass at 10μm depth of Indentation

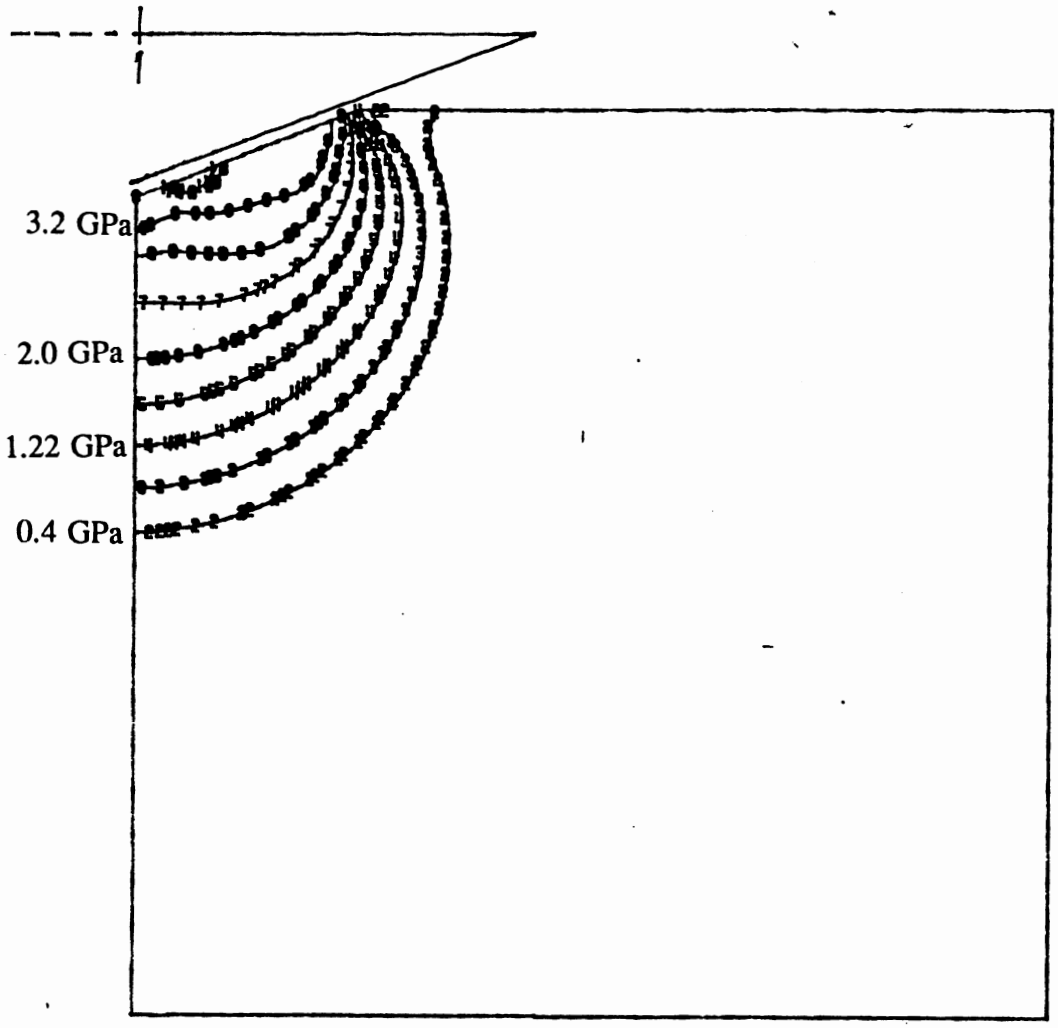

Figure 6.3 Contours of Hydrostatic Pressure in Indentation of Glass at 10μm depth of Indentation

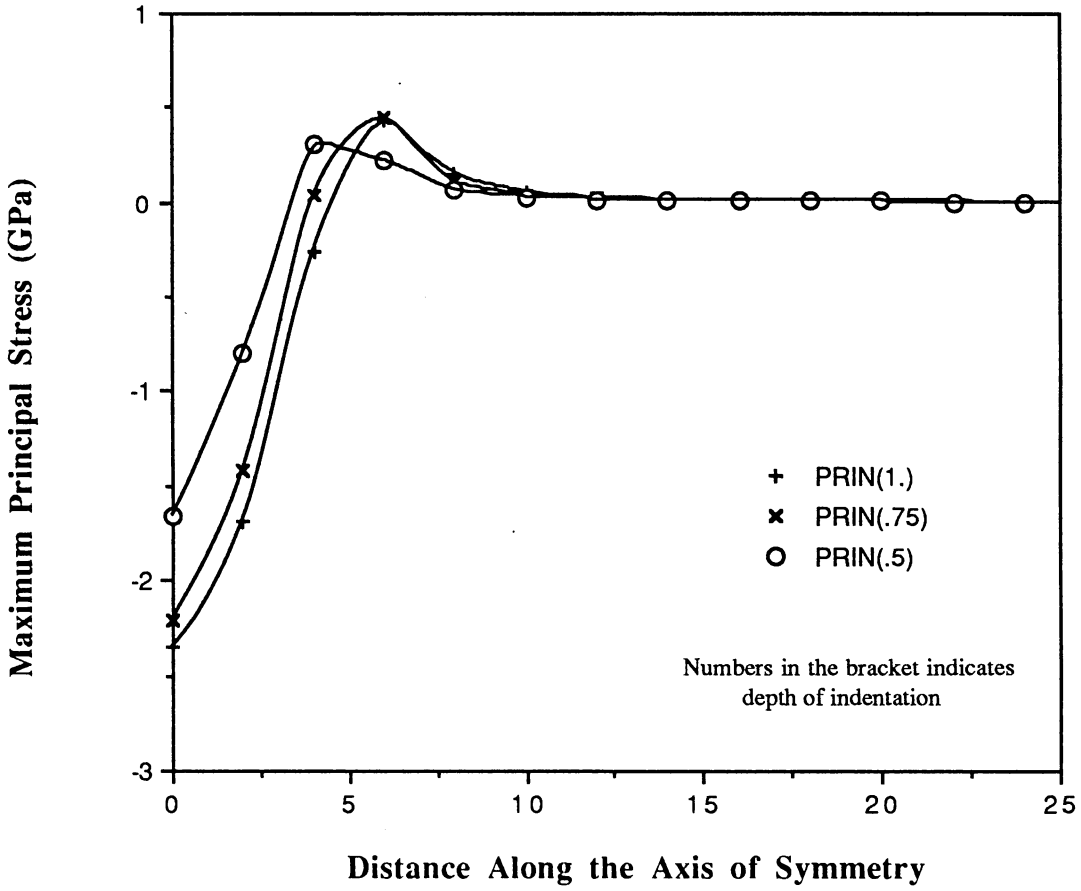

Figure 6.4 Variation of Maximum Principal Stress Along the Axis of Symmetry in Indentation of Glass for β=45°

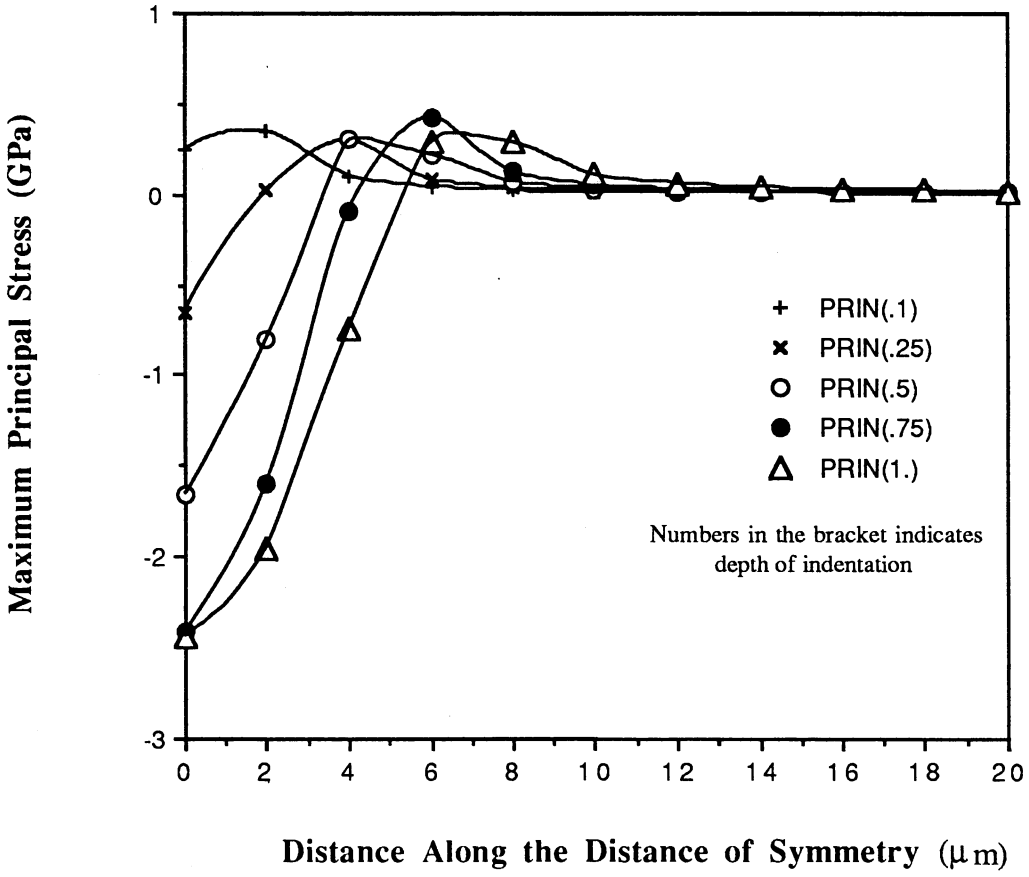

Figure 6.5 Variation of the Maximum Principal Stress Along the Axis of Symmetry in Indentation of Glass for $\beta = 22°$

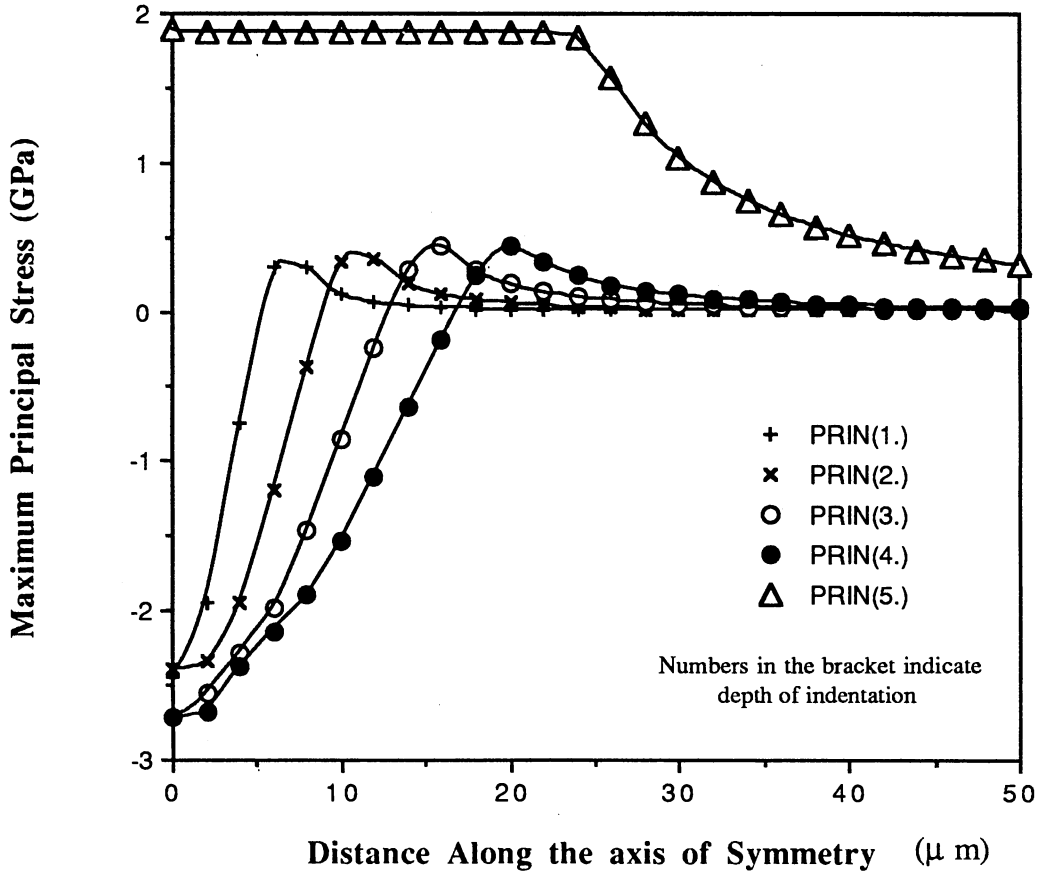

Figure 6.6 Variation in the Maximum Principal Stress with Depth of Indentation for Glass (β=22°)

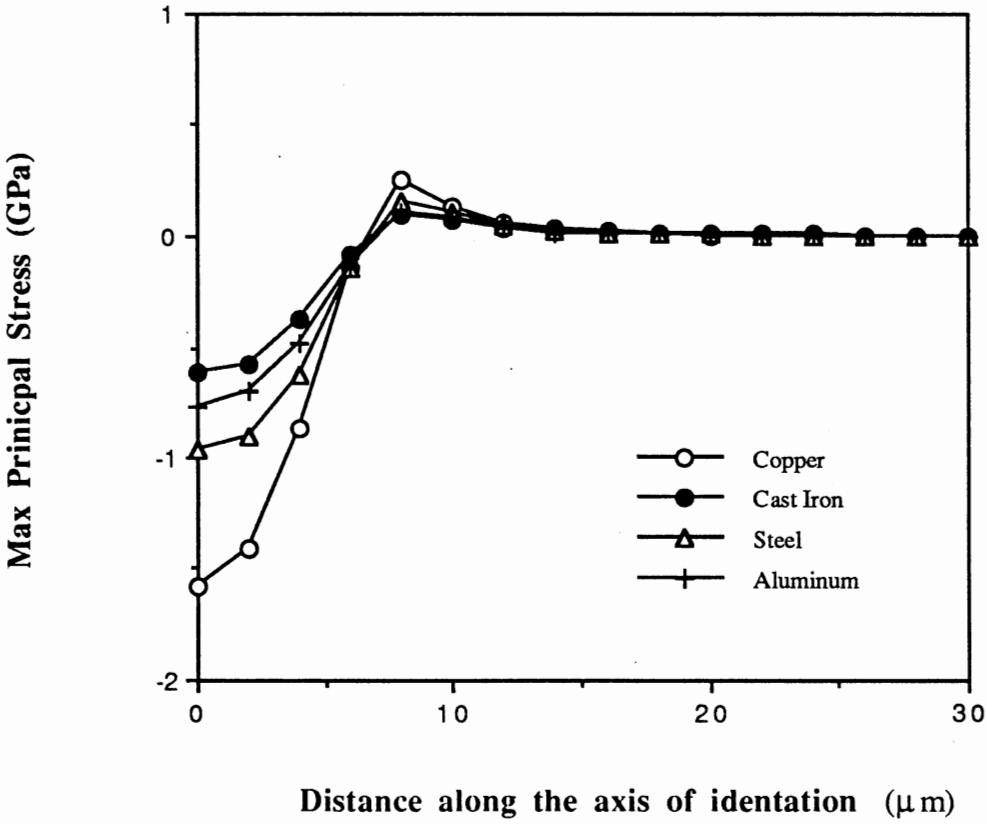

Figure 6.7 Variation in the Maximum Principal stress for various ductile materials (β=22°) at depth of indentation of 1μm

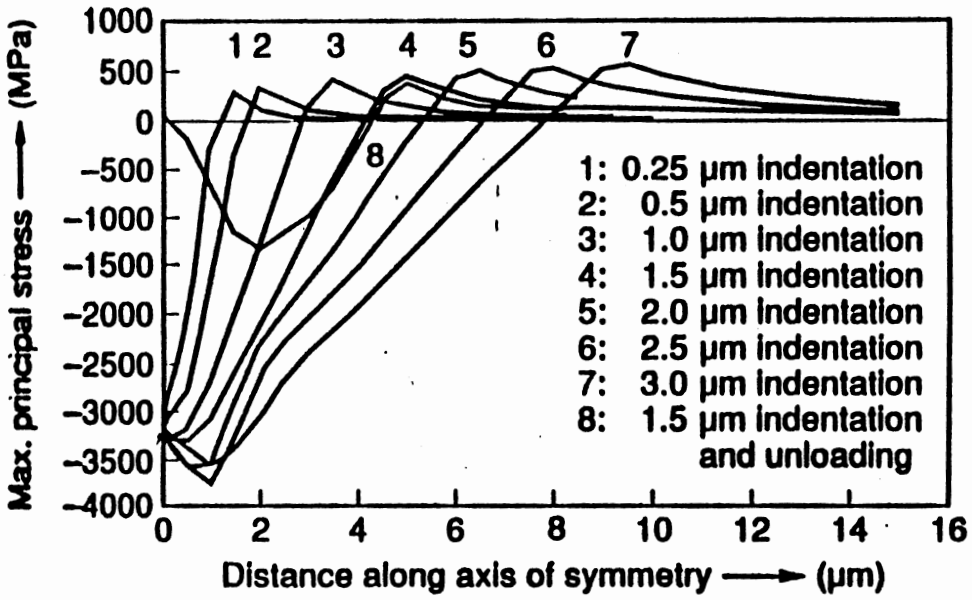

Figure 6.8 Variation of the Maximum Prinicpal Stress in Indentation of Glass at Various Depths after Franse

Y=1800 MPa and β=45°, the value of 4576 MPa for P/Y can be obtained. Franse used the average value of the maximum principal stress of ~ 3300 MPa, from Figure 6.6 (at the center of the indenter) to compare the analytical and the finite element values. He argued that the difference between the finite element and analytical value of 1276MPa (i.e 4576-3300) could be due to the effect of free surface in indentation process (refer to Figure 4.2) which is not considered in Johnson's solution. In our case, by taking the average of the hydrostatic pressure during indentation of glass with β=45° indenter, we find this difference to be (1470 MPa), which is close to the value obtained by Franse. Although Franse attributed this difference to free surface, but in reality the difference need not necessarily be attributed to the free surface. It can also be due to the compressibility of the material. Unfortunately the finite element formulation is based on elasto-plastic formulation and does not take into account the compression of the material.

Figure 6.9 and 6.10 show the variation in the hydrostatic stress along the axis of symmetry of various brittle and ductile materials respectively. From these graphs it can be observed that the hydrostatic stress is high just at the point of indentation and decreases along the axis of symmetry. This rapid increase in the hydrostatic pressure close to the indenter suggests that at small depths of grinding, the hydrostatic stress at the tip of the abrasive may be quite high. This could probably result in some plastic deformation at or near the surface. It can be observed from Figure 6.11 that the value of the maximum hydrostatic pressure is dependent on the ratio of the Young's modulus to the yield strength, decreasing with increasing value. Also, from Figure 6.9 and 6.10 it can be observed that during indentation of Al_2O_3 (E/Y=60.0) and copper (E/Y=135), the hydrostatic pressures are 11.5 and 6 GPa respectively. Hence, it can be said that brittle materials in general have higher hydrostatic pressures, beneath point of indentation, than do ductile materials.

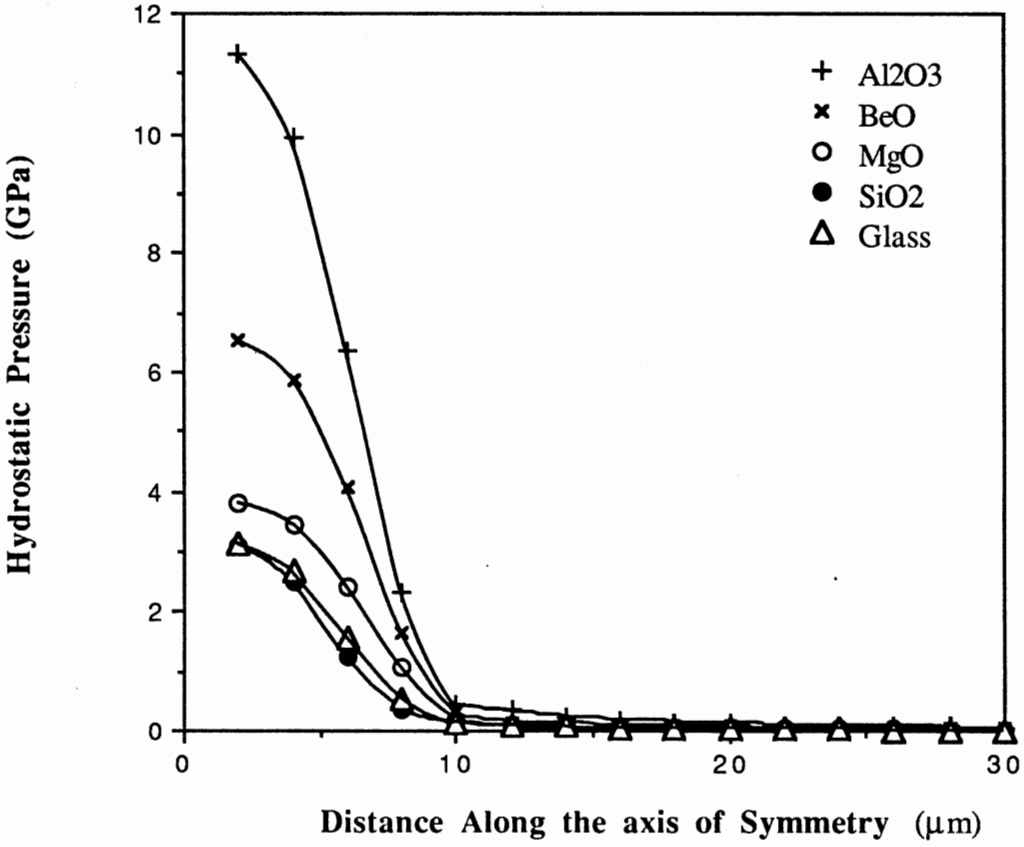

Figure 6.9 Variation in the Hydrostatic Stress Along the Axis of Symmetry in various Brittle Materials (β=22°) at 1μm depth of indentation

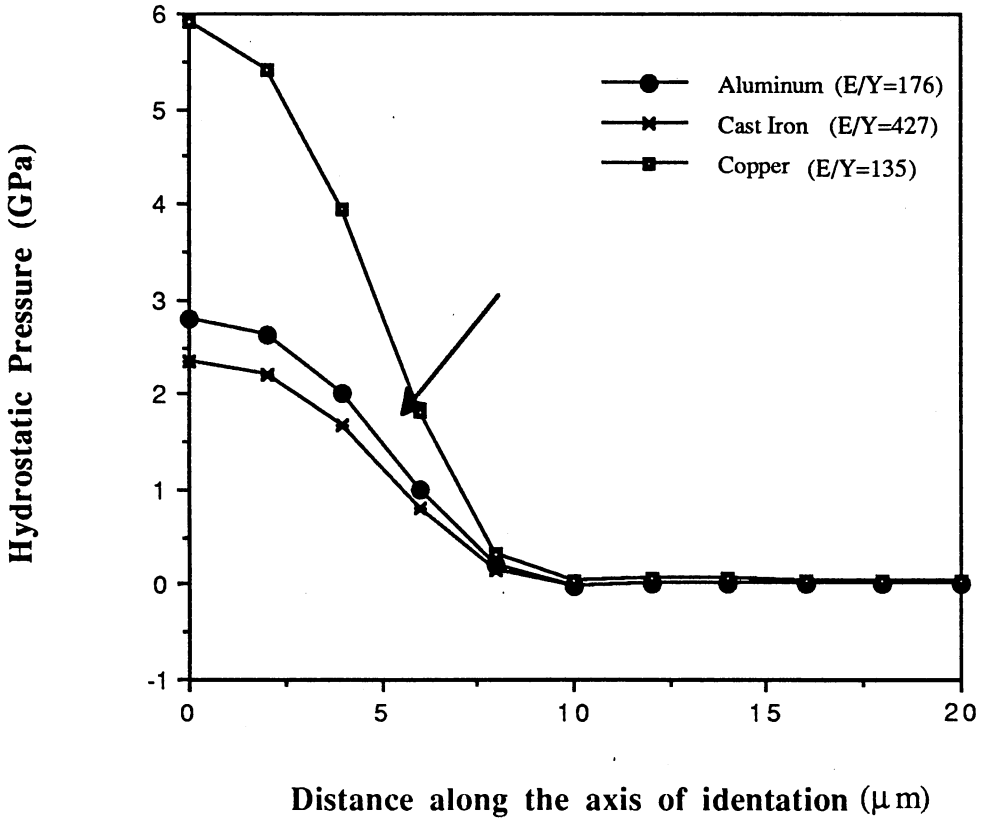

Figure 6.10 Variation in the Hydrostatic Pressure along the axis of Symmetry for various ductile materials for $\beta=22°$ and depth of indentation of 1μm

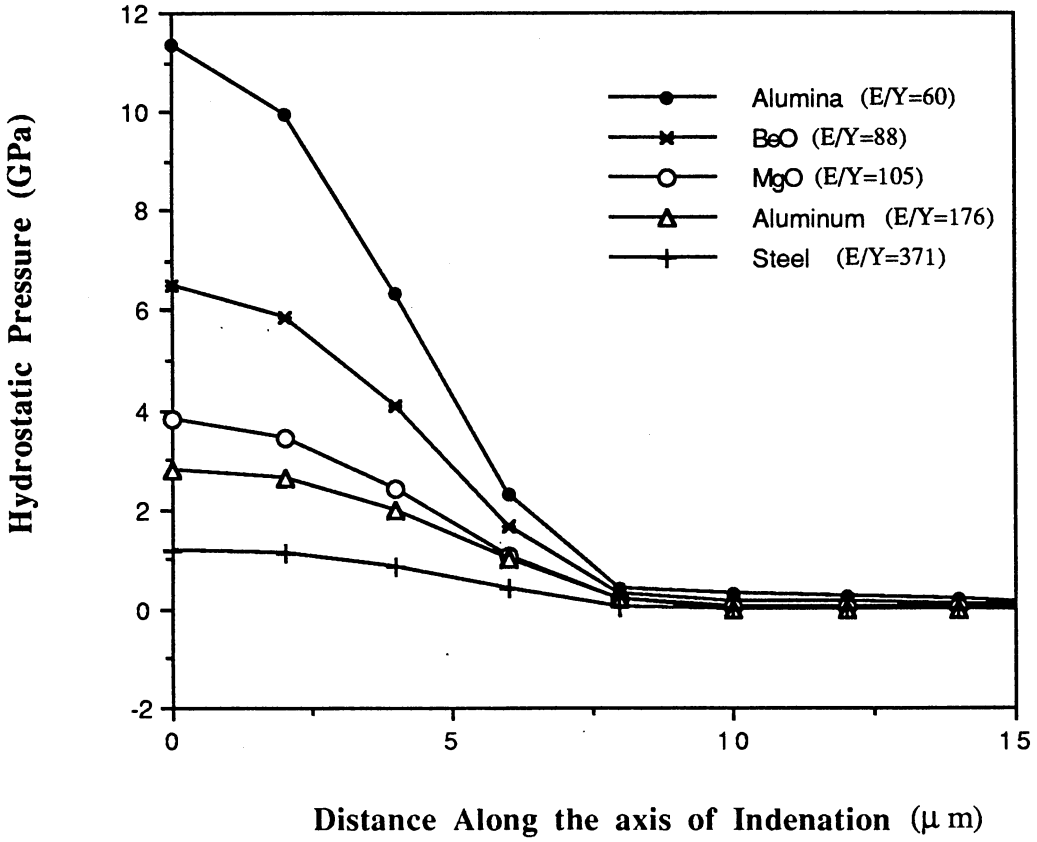

Figure 6.11 Variation in the hydrostatic pressure for various ductile and brittle materials for $\beta=22°$ and depth of indentation of 1μm

As indicated in Chapter IV, Marsh [52] working on the indentation of glass, observed that the relation of the type of P/Y~3 cannot be used for brittle materials, such as glass. Following Hill's solution he derived the following expression relating P/Y to the materials parameters, namely, E/Y.

$$\frac{P}{Y} = \frac{2}{3}\left(1 + \frac{3}{3-\lambda}\log\frac{3}{\lambda + 3\mu - \lambda\mu}\right) \tag{6.6}$$

where $\lambda = (1-2\nu)\frac{Y}{E}$ and $\mu = (1+\nu)\frac{Y}{E}$.

The above expression can also be rewritten as

$$\frac{P}{Y} = \frac{2}{3} + \frac{2}{3}B\log(Z) \tag{6.7}$$

$$\frac{P}{Y} = c + KB\log(Z) \tag{6.8}$$

where $B = \frac{3}{3-\lambda}$ and $Z = \frac{3}{\lambda + 3\mu - \lambda\mu}$

In order to evaluate the validity of the equation 6.8 and to determine the values of c and K, Marsh [52] conducted a series of experiments on derlin, glasses, and other brittle materials. From these experiments Marsh evaluated c as 0.26 and K as 0.60. In the present investigation in order to determine the value of the constants through FEM, different brittle materials such as glass, alumina, fused silica, magnesium oxide, and beryllium oxide were used. Table 6.1 lists the values of these constants for the materials using the finite element analysis of the indentation process. The results of P/Y versus the B log(z) parameter are plotted in Figure 6.12. Using this graph the values of the constants c and k were evaluated as 0.28 and 0.07 respectively. The values of constant c, it should be noted are almost equal to that of c=0.26 given by Marsh. However, the difference in the value of K many be attributed to the choice of materials. If more materials (with small and high E/Y values)

were to be chosen, then it is believed the constant K would have been closer to that given by Marsh. It may also be noted that Marsh does not indicate the value of the Young's modulus and yield strengths of various materials that he used for his experiments, and hence could not be used in the finite element.simulation.

TABLE 6.1

MATERIAL PARAMETERS B AND Z FOR VARIOUS MATERIALS

Material	ν	E/Y	λ	μ	B	Z	log(Z)
Al_2O_3	0.26	59.68	0.0080	0.02111	1.002687	42.135	3.7408
BeO	0.34	88.171	0.003629	0.01519	1.00121	61.045	4.116
MgO	0.36	105.82	0.002646	0.01285	1.00088	72.8827	4.288
SiO2	0.25	37.125	0.013460	0.04040	1.00450	22.3673	3.1076
Glass	0.26	50.0	0.0096	0.0252	1.0032	35.31153	3.5642

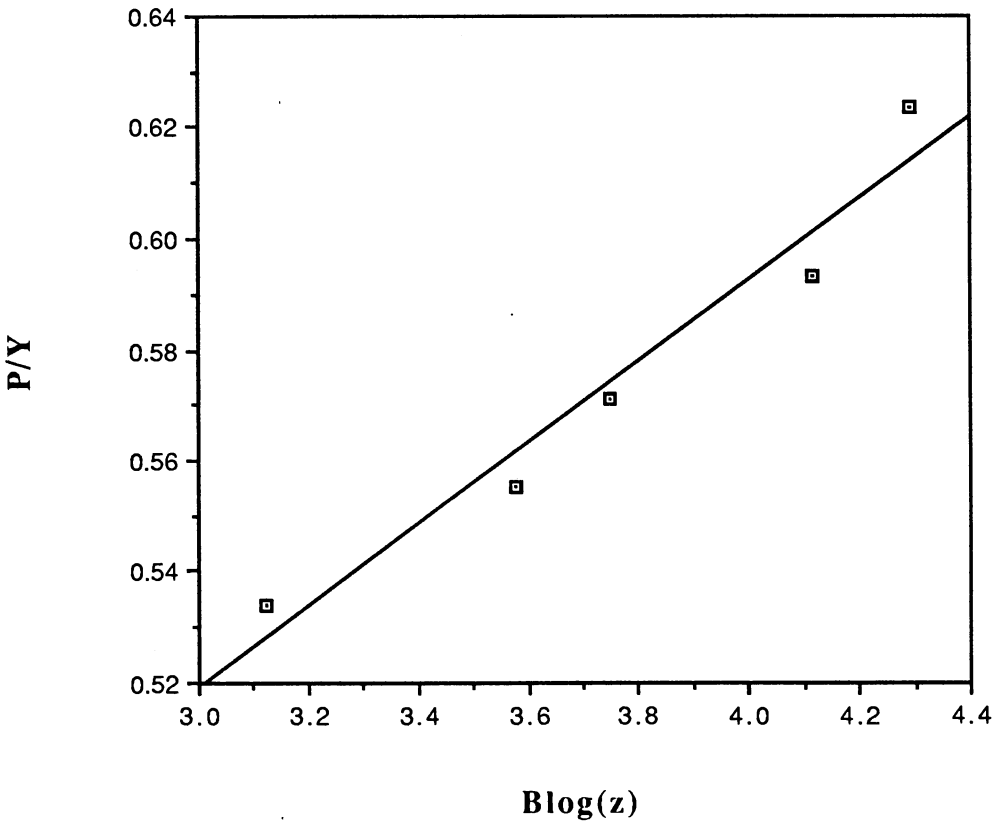

Figure 6.12 P/Y versus Material constants B and Z

CHAPTER VII

CONCLUSIONS AND RECOMMENDATIONS

In this work, the existing analytical models for the indentation of brittle materials, chiefly, the Hill's spherical cavity solution and variations of it, have been dealt in some detail. Finite element analysis of the elasto-plastic indentation problem showed that high hydrostatic pressures can be observed in regions immediately beneath the indenter [see Figure 6.3]. This high hydrostatic pressure can play a significant role in the deformation of certain brittle materials, especially glass and ceramics. Since, Hill's formulation is based on Tresca yield criterion which is applicable for ductile materials, in the present investigation this has been modified to take into account the role of first invariant of stress. Such a solution can be applied to brittle materials such as advanced ceramics. The validity of the solution, however, could not be evaluated for lack of experimental data.

The finite element analysis of the indentation of brittle materials, such as glass, alumina, magnesium oxide, fused silica, and beryllium oxide showed that the material beneath the indenter moves in radial directions. This confirms that for elasto-plastic indentation of brittle materials, the Hill's spherical cavity solution can be used. Also, as can be expected, the maximum principal stress varies along the axis of symmetry – in a small region just beneath the indenter. These stresses are highly compressive and then with increasing distance along the axis of indentation, become tensile over a very small portion before finally saturating to a zero value. It is felt that for brittle materials, this change from compressive to tensile stress could be the region where the cracking phenomenon begins to occur.

The hydrostatic pressure just beneath the indenter is high (1 ~3 GPa), and the absolute values seem to depend on the material properties especially, the ratio E/Y. Higher the value of E/Y, the lower is the hydrostatic pressure and vice versa. Since brittle materials, such as advanced ceramic materials and glass have low E/Y value, it can be expected the high hydrostatic stresses may be present during machining at low depths. However, without the experimental results it cannot be ascertained whether this high hydrostatic stresses can be successfully exploited so as to provide surfaces which are nearly crack free.

Although indentation tests provide some information on the deformation process, these results may not be directly applicable to grinding. This is because of the following : (i) indentation tests are static and do not consider the complexities associated with a dynamic process, (ii) scratch tests do provide the dynamic conditions but they are (a) carried out under constant depth of cut as opposed to the varying depth of cut in grinding process and at low speeds and (b) the stress fields are simpler and do not consider the stress interactions that arise during a grinding process, and most important of all (iii) the heat generated during the grinding process is significant and the stresses that arise because of this may also play an important role. So, the analytical solutions have to be modified so as to consider the dynamic effects.

If a true representation of the ultraprecision grinding of ceramics is to be achieved, then it is necessary to simulate the actual cutting process rather than static indentation. The finite element simulation of such a process should be able to predict whether formation of cracks take place or if plastic flow will occur. One such analysis was carried out by Ueda at al.[74] As per this formulation the stress and strain distributions in the deformation are first analyzed with FEM. Then the appropriate fracture mechanics parameters are determined. For these parameters, Ueda et al used the potential energy release rate G and the stress intensity factor K. Then the type of deformation taking place in the deformation zone of cutting is determined based on the following : if $G \geq G_c$ or $K \geq K_c$ then the material

is removed by unstable crack formation (G_c and K_c are the critical values of G and K respectively). If the above condition is not satisfied then plastic flow is assumed to take place. The above analysis can be modified for brittle materials by prescribing the yield condition that takes into account the first invariant of stress.

REFERENCES

1. Lysaght, V. E., "Indentation Hardness Testing", Reihold Publications, New York, (1949)
2. O'Neil, H., "The Hardness of Metals and Its Measurement", Sherwood Press Inc, Clevland, (1934)
3. Ponton, C. B. and R.D.Rawlings, "Vickers Indentation Fracture Toughness Test - Part I and II", Materials Science and Technology, Vol 5 (1989), pp. 865-967.
4. Blake, P. N., Bifano, T., Dow, T. and Scattergood, R. O., "Precision Machining of Ceramic Materials", Ceramic Bulletin, Vol 67 (1988), pp. 1038-1043.
5. Miyashata, M., 1st Annual Precision Engineering Conference, (1985)
6. Komanduri, R., "Unpublished Report", (1991),
7. ....."Collected Works of Bridgman", Harvard Univ. Press, Cambridge, Mass., Vol 1-7 (1964)
8. Mott, B. W., "Micro-Indentation Hardness Testing", Butterworths Scientific Publications, (1956)
9. Smith, R. L. and G.E. Sandland, "Some Notes on the Use of Diamond Pyramid for Hardness Testing", Journal of Iron and Steel Inst., Vol 3 (1925)
10. Tabor, D., "The Physical Meaning of Indention and Scratch Hardness", British Journal of Applied Physics, Vol 7 (1956), pp. 159-165.
11. Johnson, W. L., "Contact Mechanics", Cambridge University Press, (1990)
12. Dumas, G. and Barnoet, C. N., "Elasto-Plastic Indentation of Half-Space by a long Rigid Cylinder", International Journal of Mechanical Sciences, Vol 13 (1971), pp. 519-528.

13. Lee, C. H., Masaki, S. and Kobayashi, S., "Analysis of Ball Indentation", International Journal of Mechanical Sciences, Vol 14 (1972), pp. 417-424.

14. Lee, C. H. and Kobayashi, S., "Elasto-Plastic Analysis of Plane-Strain and Axisymmetric Flat Punch Indentation by the Finite Element Method", International. Journal of Mechanical Sciences, Vol 12 (1970), pp. 349-370.

15. Hardy, C., Baronet, C. N. and Tordion, G. V., "The Elasto-Plastic Indentation of Half-Space by a Rigid Sphere", International Journal for Numerical Methods in Engineering, Vol 3 (1971), pp. 451-462.

16. Hill, R., Lee, E. H. and Tupper, S. J, "The Theory of Wedge Indentation of Ductile Metals", Proc. Royal Soc., Vol A188 (1947), pp. 273-280.

17. Johnson, W. and P.B. Mellor, "Engineering Plasticity", Ellis Horwood Ltd. (1983)

18. Samuels, L. E., "Microindentation of Metals", in Microindentation Techniques in Materials Science in ASTM STP 889, (1986), pp. 5-25.

19. Grunzweig, J., Longman, I. M. and Petch, N.J., "Calculations and Measurements on Wedge Indentation", Journal of the Mechanics and Physics of Solids, Vol 2 (1954), pp. 81-86.

20. Mulheran, T. O., "Deformation of Metals by Vickers-type Pyramidal Indenters", Journal of Mechanics and Physics of Solids, Vol 7 (1959), pp. 85-96.

21. Samuels, L. E. and Mulheran, T. O., "The Deformation Zone Associated with Indentation Hardness Impression", Journal of Mechanics and Physics of Solids, Vol 5 (1956), pp. 125-132.

22. Kelly, K., "Strong Solids", Oxford, Clarendon, (1966)

23. Dieter, G., "Mechanical Metallurgy", McGrawHil Publ., (1988)

24. Kelly, A., "Ductile and Brittle Crystals", Phil. Mag., Vol 15 (1967), pp. 567-585.

25. Lawn, R., "Fracture of Brittle Solids", Cambridge University Press, New York, (1975)

26. Gogotsi, G. A., Groushevsky, Y. L. and Strelov, K. K., "The Significance of Non-Elastic Deformation in the Fracture of Heterogeneous Ceramic Materials", Ceramurgia International, Vol 4 (1978), 3, pp. 113-117.

27. Bridgman, P. W. and I.Simons, "Effects of Very High Pressure on Glass", Journal of Applied Physics, Vol 24 (1953), 4, pp. 405-413.

28. Lawn, B. R. and Wilshaw, R., "Indentation Fracture : Principles and Applications", Journal of Materials Science, Vol 10 (1975), pp. 1049-1081.

29. Peter, K. W., "Densification and Flow Phenomenon of Glass in Indentation Experiments", Journal of Non-Crystalline Solids, Vol 5 (1970), pp. 103-115.

30. Zhang, B., Tokura, H. and Yoshikawa, M., "Study of Surface Characteristics of Non-Oxide Ceramics Scratched by Single Point Diamonds", Japan Society of Precision Eng., (1988), pp. 159-146.

31. Timoshenko, S. P. and D.A. Goodier, "Theory of Elasticity", McGraw-Hill Publ. (1983)

32. Evans, A. G., in "The Science of Ceramic Machining and Surface Finishing II " ed NBS Special Publications # 562, (1979), pp. 1-14.

33. Bridgman, P. W., "The Effect of Hydrostatic Pressure on the Fracture of Brittle Substances", Journal Applied Physics, Vol 18 (1947), pp. 246-258.

34. Bridgman, P. W., "The Tensile Properties of Several Special Steels and certain other Materials Under Pressure", Journal of Applied Physics, Vol 17 (1946), pp. 201-212.

35. Bifano, T. G., "Ductile Regime Grinding of Brittle Materials", PhD Thesis, Dept. of Mechanical Eng. , North Carolina State University, (1988)

36. King, K. K. and Tabor, D., "The Strength Properties and Frictional Behavior of Brittle Solids", Proc. of Royal Soc. of London, Vol A 223 (1954), pp. 225-238.

37. Brace, W. F., "Behavior of Quartz During Indentation", Journal Geology, (1962), pp. 581-595.

38. Warren, R. and Matzke, H., "Indentation of a Broad Range of Cemented Carbides", in Science of Hard Materials ed by Vishwanadham, R.K, Rowcliffe and J. Gurland, Plenum Press, New York, (1981), pp. 563-581.

39. Warren, R., "Measurement of Fracture Properties of Brittle Solids by Hertzian Indentation", Acta. Mettalurgia, Vol 26 (1978), pp. 1759-1769.

40. Rowcliffe, D.J, "Indentation damage in Tungsten Carbide and Tungsten-Titanium Carbide", in Science of Hard Materials ed. by Vishwanadham, R.K., Rowcliffe D.J, and J.Gurland, Plenum Press, New York, (1981), pp. 155-168.

41. Puttick, K. E., "The Indentation of Perspex", Journal of Physics :E, Vol 6 (1973), pp. 116-118.

42. Puttick, P. E., Smith, L. S. A. and Miller, L. E., "Stress fields Around Indentation of PMMA", Journal of Physics :D, Vol 1977 (1977), pp. 617-631.

43. Puttick, K. E., Shahid, M. A. and Hosseini, M. M., "Size Effects in Abrasion of Brittle Materials", Journal of Physics : D, Vol 12 (1979), pp. 195-202.

44. Puttick, K. E., "The Correlation of Fracture Transitions", Journal of Applied. Physics:D, Vol 13 (1980), pp. 2249-2262.

45. Puttick, K. E., Rudman, M. R., Smith, K.J, Franks, A. and K.Lindsey, "Single Point Diamond Machining of Glass ", Proc. of Royal Soc., Vol A420 (1989), pp. 19-31

46. Veldkamp, J. D. B. and Wassink, R. J.K., "Grindability of Brittle Materials : A Theoretical and Experimental Investigation", Philips Research Review, Vol 31 (1970), pp. 153-189.

47. Blake, P. N. and Scattergood, R. O., "Ductile-Regime Machining of Germanium and Silicon", Journal of American Ceramic Society, Vol 74 (1990), pp. 949-957.

48. Kendall, K., "Complexities of Compression Failure", Proc. of Royal Soc., Vol A 361 (1978), pp. 245-263.

49. Taylor, E. W., "Plastic Deformation of Optical Glass", Nature, (1949), pp. 223.

50. Ainsworth, L., "The Diamond Pyramid Hardness Hardness of Glass in Relation to the Strength and Structure of Glass, Part I,II and III", Journal Soc. Glass Tech., Vol 38 (1954), pp. 480-499T.

51. Tabor, D., "The Hardness of Solids", (1970), pp. 145-179.

52. Marsh, D., "Plastic Flow in Glass", Proc. of Royal Soc. of London, Vol 279 (1964), pp. 420-430.

53. Hagan, J.T., "Shear Deformation under Pyramidal Indentations in Soda Lime Glass", Journal of Material Science, Vol 15 (1980), pp. 1417-1424.

54. Huerata, H. and Malkin, S., "Grinding Glass : The Mechanics of the Process", ASME, Journal of Eng. for Industry, (1976), pp. 459-467.

55. Kirchner, H. P., "Comparison of Single Point and Multipoint Grinding Damage in Glass", Journal of American Ceramic Society, Vol 67 (1984), pp. 347-353.

56. Ernsberger, F. M., "Mechanical Properties of Glass", Journal of Non-Crystalline Solids Vol 1 (1969), pp. 295-321.

57. Sakka, S. and MacKenzie, J. D., "High Pressure Effects on Glass", Journal of Non-Crystalline Solids, Vol 1 (1969), pp. 107-142.

58. Finnie, I. H., "On Machining Glass", Journal of Materials Science, Vol 13 (1980), pp. 2508-2513.

59. Loubet, J.L., Georges, J. M. and Meille, G., "Vickers Indentation Curves of Elastoplastic Materials", in Microindentation Techniques in Materials Science in ASTM STP 889, (1986), pp. 72-89.

60. Hill, R., "Mathematical Theory of Plasticity", Cambridge University Press (1950), pp. 99-105

61. Johnson, K. L., "The Correlation of Indentation Experiments", Journal of Mech. and Physics of Solids, Vol 18 (1970), pp. 115-126.

62. Chiang, S. S., Marshall, D. B. and Evans, A. G., "The Response of Solids to Elastic/Plastic Indentation I and II", Journal of Applied Physics, Vol 53 (1982), Jan, pp. 298-317.

63. Mindlin, R. D., "Force at a Point in the Interior of a Semi-Infinite Solid", Journal. Applied. Physics, Vol 7 (1936), pp. 195-202.

64. Bridgman, P. W., "Effects of Very High Pressure on Glass", Journal of Applied. Physics, Vol 24 (1953), April, pp. 405-413.

65. Bridgman, P. W., "The Effect of Pressure on the Tensile Properties of Several Metals and Other Materials", Journal of Applied Physics, Vol 24 (1953), May, pp. 560-570.

66. Vodar, B. and Kiefer, J, "Historical Introduction", in Mechanical Behavior of Materials under Pressure, Elsevier Publ., New York, (1970), pp. 1-45.

67. Pugh, M., "Mechanical Properties of Materials under Pressure", in Mechanical Behavior of Materials under Pressure, Elsevier Publ., New York, (1970), pp. 236-272.

68. Drucker, D. C. and Prager, W., "Soil Mechanics and Plastics Analysis or Limit Design", Quart. Applied. Mathematics, Vol 10 (1952), pp. 157-165.

69. Green, R. J, "A Plasticity Theory for Porous Solids", Int. Journal Mechanical Sci., Vol 14 (1972), pp. 215-224.

70. Im, Y.T., "Finite Element Modelling of Plastic Deformation of Porous Materials", PhD. Dissertation, University of California (Berkley), 1985.

71. Chen, I. W., "Implication of Transformation Plasticity in ZrO2-Containing Ceramics : II, Elastic-plastic Indentation", Journal of American Ceramic Society, Vol 69 (1986), March, pp. 189-194.

72. Yasui, I. and Imoka, M., "Analysis of Indentations of glass by FEM", 10th Int. Congr. on Glass, Kyoto (Japan) 1974, (1974), pp. 53-60.

73. Franse, J, "Aspects of Precision Grinding", PhD Thesis at Technische Universiteti (Netherlands), (1991).

74. Ueda,K , Sugita, T, and H.Tsuwa, Annals of CIRP Vol 32 1983

VITA 2

VENKATA CHANDRA MOULI VISSA

Candidate for the Degree of

Master of Science

Thesis: AN ANALYSIS OF INDENTATION OF BRITTLE MATERIALS

Major Filed : Mechanical Engineering

Biographical

Personal Data: Born in Hyderabad, Andhra Pradesh, India, March 15th, 1964, the son of Hanumantha Rao and Kapalkavalli.

Education: Received Bachelor of Engineering degree in Mechanical Engineering from Andhra University, Andhra Pradesh, India in July 1986; completed requirements for the Master of Science degree at Oklahoma State University in December 1992.

Professional Experience : Assistant Engineer Purchase, Hyderabad Allwyn Ltd.(Watch Division) , Hyderabad, India, December 1986 to December 1989; Research Assistant Department of Mechanical and Aerospace Engineering, Oklahoma State University, January 1990 to August 1992.